Quaternary Science Reviews 72 (2013) 83–107

Contents lists available at SciVerse ScienceDirect

Quaternary Science Reviews

journal homepage: www.elsevier.com/locate/quascirev

Reassessing the evidence for tree-growth and inferred temperature change during the Common Era in Yamalia, northwest Siberia

Keith R. Briffa [a,*], Thomas M. Melvin [a], Timothy J. Osborn [a], Rashit M. Hantemirov [b], Alexander V. Kirdyanov [c], Valeriy S. Mazepa [b], Stepan G. Shiyatov [b], Jan Esper [d]

[a] Climatic Research Unit, School of Environmental Sciences, University of East Anglia, Norwich NR4 7TJ, UK
[b] Institute of Plant and Animal Ecology, Ural Branch of the Russian Academy of Sciences, 8 Marta Street 202, Ekaterinburg 620144, Russia
[c] V.N. Sukachev Institute of Forest, Siberian Branch of the Russian Academy of Sciences, Akademgorodok, Krasnoyarsk 660036, Russia
[d] Department of Geography, Johannes Gutenberg-University, 55099 Mainz, Germany

ARTICLE INFO

Article history:
Received 20 December 2012
Received in revised form
9 April 2013
Accepted 10 April 2013
Available online 24 May 2013

Keywords:
Dendroclimatology
Climate reconstruction
Medieval Warm Period
Polar Urals
Yamal
Summer temperature

ABSTRACT

The development of research into the history of tree growth and inferred summer temperature changes in Yamalia spanning the last 2000 years is reviewed. One focus is the evolving production of tree-ring width (TRW) and tree-ring maximum-latewood density (MXD) larch (*Larix sibirica*) chronologies, incorporating different applications of Regional Curve Standardisation (RCS). Another focus is the comparison of independent data representing past tree growth in adjacent Yamalia areas: Yamal and Polar Urals, and the examination of the evidence for common growth behaviour at different timescales. The sample data we use are far more numerous and cover a longer time-span at Yamal compared to the Polar Urals, but Yamal has only TRW, while there are both TRW and MXD for the Polar Urals. We use more data (sub-fossil and from living trees) than in previous dendroclimatic studies in this region. We develop a new TRW chronology for Yamal, more than 2000 years long and running up to 2005. For the Polar Urals we develop new TRW and MXD chronologies that show good agreement at short (<15 years) and medium (15–100 years) timescales demonstrating the validity of attempts to reconcile the evidence of longer-timescale information that they provide. We use a "conservative" application of the RCS approach (two-curve signal-free RCS), guarding against the possibility of "modern sample bias": a possible inflation of recent chronology values arising out of inadvertent selection of mostly relatively fast-growing trees in recent centuries. We also transform tree indices to have a normal distribution to remove the positive chronology skew often apparent in RCS TRW chronologies. This also reduces the apparent magnitude of 20th century tree-growth levels.

There is generally good agreement between all chronologies as regards the major features of the decadal to centennial variability. Low tree-growth periods for which the inferred summer temperatures are approximately 2.5 °C below the 1961–90 reference are apparent in the 15-year smoothed reconstructions, centred around 1005, 1300, 1455, 1530, particularly the 1810s where the inferred cooling reaches −4 °C or even −6 °C for individual years, and the 1880s. These are superimposed on generally cool pre-20th century conditions: the long-term means of the pre-1900 reconstructed temperature anomalies range from −0.6 to −0.9 °C in our alternative reconstructions. There are numerous periods of one or two decades with relatively high growth (and inferred summer temperatures close to the 1961–1990 level) but at longer timescales only the 40-year period centred at 250 CE appears comparable with 20th century warmth. Although the central temperature estimate for this period is below that for the recent period, when we take into account the uncertainties we cannot be highly confident that recent warmth has exceeded the temperature of this earlier warm period. While there are clear warm decades either side of 1000 CE, neither TRW nor MXD data support the conclusion that temperatures were exceptionally high during medieval times. One previous version of the Polar Urals TRW chronology is shown here to be in error due to an injudicious application of RCS to non-homogeneous sample data, partly derived from root-collar samples that produce spuriously high chronology values in the 11th and 15th centuries. This biased

* Corresponding author.
E-mail address: k.briffa@uea.ac.uk (K.R. Briffa).

http://dx.doi.org/10.1016/j.quascirev.2013.04.008

chronology has been used in a number of recent studies aimed at reconstructing wider scale temperature histories. All of the chronologies we have produced here clearly show a generally high level of growth throughout their most recent 80 years. Allowing for chronology and reconstruction uncertainty, the mean of the last 100 years of the reconstruction is likely warmer than any century in the last 2000 years in this region.

1. Introduction and study objectives

This paper describes a consolidation and reanalysis of the evidence for past tree-growth and inferred temperature changes provided by tree-ring width (TRW) and maximum latewood density (MXD) chronologies spanning up to 1200 years in the north-eastern Ural Mountains and the last 2500 years in the adjacent southern Yamal Peninsular region of northwest Siberia. The whole study area corresponds to the western part (henceforth "Yamalia") of the Yamal-Nenets Autonomous Area of Russia whose administrative centre is Salekhard. The tree-ring data from this wider Yamalia region are important because various subsets, processed in different ways, have been used to infer past local temperature changes in previous publications (Shiyatov, 1962; Graybill and Shiyatov, 1989; Briffa et al., 1995; Esper et al., 2002). Chronologies from this region have also been included as predictor data in reconstructions of Northern Hemisphere average temperature changes through the last ~1200 years (e.g. Mann and Jones, 2003). Similar and additional data to those analysed here are likely to contribute to ongoing efforts to characterise the spatial patterns of past temperature variability in high northern latitudes and average changes at hemispheric or global geographic scales. Higher-latitude regions of the Northern Hemisphere have warmed faster than most other regions of the world (Serreze et al., 2009) and numerical climate models indicate that future warming at these latitudes under enhanced greenhouse gas conditions is also likely to outpace that experienced at lower latitudes in the medium term (e.g. Fig. 4 of Joshi et al., 2011). However, the strength of the feedbacks that amplify changes in this region, and thus the magnitude and seasonality of Arctic amplification, are uncertain (Holland and Bitz, 2003) and improved records of past temperature changes in the circum-Arctic region are needed to expand our knowledge. One objective of the present study is to review the evidence for the timing and relative magnitude of circa medieval versus recent warmth. This topic is of considerable interest both regionally and globally in the context of attempts to attribute causes for past and projected future climate changes (Goosse et al., 2012; Schurer et al., 2013).

Assessing the value of tree-ring data for climate reconstruction is predicated on an understanding of the methods of tree-ring chronology production and the extent to which these methods affect the estimation of uncertainty. At issue is the representation of the tree-ring evidence itself, but also the implementation of specific regression or scaling techniques used to transform the tree-ring data into estimates of climate variability. Fundamental to this review is an exploration of the degree to which the different tree-ring variables and sub-sets of these data provide consistent, and hence mutually corroborative, evidence of inferred temperature changes. These issues are illustrated and discussed, and then an updated, consolidated description of the evidence of summer temperature variability for the last 2000 years in northwest Siberia is presented.

2. Review structure

The research into the variability of past tree growth in Yamalia has been focussed principally at locations in two adjacent areas (Fig. 1): the first is the upper tree-line on the eastern flank of the Polar Urals. The second is at various locations near the current latitudinal tree-line on the Yamal Peninsula, some 200 km north-east of the Polar Urals. Previous studies, using both living and dead (sub-fossil and relict) wood samples from these two areas, have provided evidence of the predominant summer temperature influence on the year-to-year growth of trees in this region and have produced millennial-scale histories of inferred changing summer temperatures for both areas (Shiyatov, 1986; Graybill and Shiyatov, 1989; Briffa et al., 1995; Shiyatov, 1995; Hantemirov and Surkov, 1996; Hantemirov and Shiyatov, 2002).

Here, we first explain the underlying concepts and dendroclimatological methods that are of particular importance to this reassessment. We next review and reanalyse currently available tree-ring data from Yamal (these are TRW data only). We then review the past and current status of the Polar Urals TRW and MXD

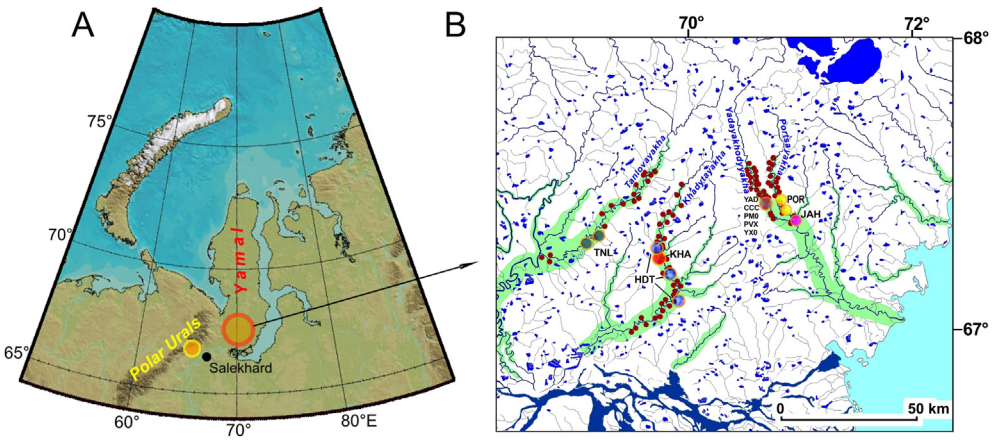

Fig. 1. The "Yamalia" (Yamal Peninsula and Polar Urals) region, showing (A) the general locations of the two study areas and (B) a detailed map of the southern part of the Yamal Peninsula. Brown points mark the main locations where sub-fossil wood has been found (identification of the labels appears in SM2 Table YT1). Salekhard is the location of the meteorological station used in this study. (For interpretation of the references to colour in this figure legend, the reader is referred to the web version of this article.)

data and compare the evidence from both variables and both areas. We explore the statistical comparison of the combined, wider regional tree-growth changes and the observed instrumental evidence of recent climate variability at different timescales. Finally we draw conclusions about inferred temperature changes over the last one to two millennia.

Extensive Supplementary Material (SM) is also provided to document many more details concerning the tree-ring data, temperature data, and the multiple stages of data processing and analysis. These are also available along with various measurement data and chronologies produced, at http://www.cru.uea.ac.uk/cru/papers/briffa2013qsr/ and numerous references to these SM are made at appropriate points within the main text.

3. Background concepts

It is implicit in dendroclimatology that parallel tree-ring data series extracted from adjacent trees exhibit common variations in time that represent the local tree-growth response to changing environmental influences. The construction of regional tree-ring chronologies, incorporating data taken from multiple trees, is intended to express the net underlying pattern of these environmental influences from year to year, decade to decade and century to century. The strength of environmental control can be gauged at a local scale by measuring the degree of correspondence shown among parallel series of measurements; typically a group of trees growing in close proximity show a common growth "signal", and the statistical quality of the chronology is assessed by comparing the expression of this signal against the measurement of associated "noise", i.e. the proportion of random variance obscuring the expressed signal in any part of the chronology (Wigley et al., 1984; Briffa and Jones, 1990).

At the local geographic scale it is often the case that the strength of the underlying common variability expressed in a tree-ring chronology is greatest at short timescales, as represented at the inter-annual to decadal timescale, with multi-decadal and longer timescales of variation showing generally lower levels of common variability. When assessing the degree of intra-regional agreement between tree-growth patterns, it is also informative to compare tree-ring chronologies with respect to specific timescales of information. By using simple high- and low-pass digital filters we can decompose the tree-ring evidence both within and between local sites into discrete classes representing "short" (here defined as changes in variability occurring over periods less than 15 years), "medium" (between 15 and 100 years) and "longer" (greater than 100 years) timescales. Where there is a presumption of similar climate control on tree growth we would expect to see similar patterns of variability in different sub-samples of a data set for each timescale.

4. Statistical processing of tree-ring data

4.1. Regional Curve Standardisation

Series of radial TRW or MXD measurements must be 'standardised' to remove long-timescale variations that represent systematic patterns of growth associated with changing tree geometry rather than the influence of any external environmental factors (Fritts, 1976, p246–311). Some standardisation methods do not discriminate between climate and non-climate influences on tree growth and remove all long-timescale variation in measured growth series, typically eliminating all evidence of climate change on timescales equal to or greater than the life spans of the sampled trees (Cook et al., 1995; Briffa et al., 1996). However, the Regional Curve Standardisation (RCS) approach has the potential to preserve long-timescale information (Briffa et al., 1992; Esper et al., 2002, 2003; Büntgen et al., 2005; Cook et al., 2006; D'Arrigo et al., 2006; Briffa and Melvin, 2011).

RCS involves the estimation of a statistical function representing the expected value of growth measurement as a function of tree age, for a particular tree species growing in a particular region. This function is derived empirically as the average of many sample measurements from trees that grew during different time periods, aligned according to their relative life stage i.e. with respect to years after the tree reaches sampling height. Using simple one-curve RCS, samples need to be drawn from a wide range of calendar dates in order for the averaging process to minimise any variation of the RCS curve produced by changing climate (Briffa et al., 1992). The derived, smoothed function of expected TRW (or MXD) represents the non-climatic influence on measured growth and is used to remove this influence from the original TRW (MXD) measurement series. This is simply achieved by dividing the measured values by the expectation for the appropriate ring-age given by the RCS curve. The resulting dimensionless "tree indices" are then averaged in their correct calendar alignment to produce a "standardised" chronology.

To date the RCS approach is arguably the most promising one for processing tree-ring data where the representation of long-timescale growth changes is an important consideration. RCS preserves long-timescale signal variance in temporal changes of the means of series of standardised tree indices, each of which is set relative to the magnitude of the RCS curve. RCS preserves medium-frequency variance in the slope of each series of tree indices which is set relative to the slope of the RCS curve. To extract accurate long-timescale changes in growth rates using the RCS approach requires many more samples than for the extraction of high-frequency variance.

4.2. Multiple RCS curves

The simple RCS approach relies on the assumption that a common, single RCS function is appropriate to detrend all measured series. This assumption may not be valid, even for trees within a restricted area. Part of the observed reduction of ring width with increasing tree age is due to the change in stem diameter, which is actually dependent on growth rate rather than ring age, e.g. the reduction of measured ring-width in each year due to diameter change will be larger in fast-growing trees than in slow-growing trees. There is usually some random variation in the growth rates of trees at a site even under constant climate conditions (Fritts, 1976, p280). It is on top of this natural variation that changes in the environmental (i.e. climate) forcing of tree growth adjusts the proportion of slow and fast growing trees over time.

Sampling trees from different sites across a region may produce bias in the common signal of an RCS chronology due to local site differences (e.g. soil or aspect). Where the type or relative counts of samples from different contexts (e.g. sub-fossil trees, archaeological samples or living-tree samples) change over time it is important to investigate whether any changes in the derived common tree-growth signal are not simply the result of changes in relative sample context i.e. that they do not represent samples from different statistical populations. It is necessary to test whether the sub-groups have systematic differences in their mean index values after taking care to allow for expected differences associated with the influence of varying ring ages and that of climate (Melvin et al., 2013; SM4). Where systematic differences between sub-groups are found, the ring measurements should either be scaled to remove the identified bias prior to their being combined into a single data set or, where this will not resolve the problem, the sub-groups should be standardised separately

(Melvin et al., 2013). A particular problem is also associated with the widespread tendency for samples from living trees to be preferentially taken from competitionally-dominant or obviously large trees. This can lead to "modern-sample bias" where the resulting disproportionately larger number of relatively faster growing (as opposed to slower growing and hence small) younger trees produces a positive bias in the recent section of the chronology (Briffa and Melvin, 2011).

If all measured series being considered are first converted into series of tree indices based on the use of one RCS curve, the indices can be sub-divided (either randomly or according to some criterion such as sample source classification or mean growth rate) and the sub-groups of index series averaged to form sub-chronologies that can then be inter-compared to reveal any systematic differences that might indicate potential bias. Major differences in sub-chronology slopes indicate the need to use different-shaped RCS curves for each sub-group of data, while major differences in means show the need to use one or more (growth-rate based) RCS curves to standardise the combined group.

By comparing the sub-chronologies, each standardised using its own RCS curve, it is possible to assess the ability of RCS processing methods to recover the same common tree-growth forcing signal from different sets of trees (Esper et al., 2002; Melvin, 2004; Melvin et al., 2013). Provided there are sufficient trees, separate (multiple) RCS curves can be developed for a variety of data sub-divisions, including those representing different growth rate classes, from the same source of trees (Erlandsson, 1936; Melvin, 2004). This will often reduce the overall chronology uncertainty and mitigate against bias created when a poorly fitting single RCS curve is used to standardise different sample data (or data from different growth-rate classes). However, the mean value across all tree indices within a particular sub-class will be approximately 1.0 after standardising the samples with the RCS curve estimated using the measurements from trees in that class. Unless differences in the mean values of the various sub-chronologies are re-instated some of the longest-timescale variance may be lost, although some changes in tree-growth rate can be preserved in the slopes of tree indices. There is generally a trade off when using multiple RCS curves: they can reduce systematic sampling bias but using too many may result in some loss of low-frequency variance. This can be seen in the limit of having a separate RCS curve for each individual sample, which is equivalent to curve-fitting standardisation that removes all low-frequency variance because the mean of each tree index series is set to 1.0 and the temporal trend of each series is removed.

In this reassessment we place considerable emphasis on the practical application of single and multiple-RCS for processing the currently available Yamalian tree-ring width and density data. Specifically, we examine the possibility of sampling bias over time, particularly the possibility of 'modern sample bias', and assess the high, medium and low-frequency confidence associated with the TRW and MXD chronologies from this region.

4.3. Signal-free standardisation

A conceptual model for a tree-ring measurement series is that it combines variations in the tree parameter seen as a change in value with tree age (or size), an environmental (e.g. climate) signal that is common to the sample of trees being considered, and other variations (typically considered to be noise) that affect individual tree series differently. Traditionally, the first of these three effects is estimated and removed via standardisation and then a chronology is subsequently formed (by averaging the tree indices) to provide the best estimate of the underlying common signal. Melvin (2004) and Melvin and Briffa (2008) introduced a method that allows the simultaneous estimation of the standardisation growth curve and the chronology together. This iterative method removes the influence of the common (assumed climate) signal on the standardisation growth curve, which reduces the "trend distortion" that can occur near the ends of a traditionally-standardised chronology. This "signal-free" standardisation can be applied to both curve-fitting and RCS standardisation (Briffa and Melvin, 2011; Melvin and Briffa, 2013a), and throughout this study we have used signal-free RCS standardisation (SF RCS).

4.4. Transformation of tree indices

Tree indices are obtained by the division of measurement data by the appropriate age values of the RCS curve. The tree indices have an asymmetric (and hence non-normal) distribution because the lower measurement values are bounded at zero while the upper values are comparatively unbounded. This asymmetry (positive skew) carries over to the chronology formed as the average of the tree indices. Here, we pool the tree index values across all years and across all the samples in a given chronology, rank them by magnitude, and then replace each index value with the value from a set of the same total number of values drawn from a standard normal distribution that has the same relative rank position (Melvin and Briffa, 2013a,b). The tree indices are thus transformed to have a normal distribution, and here we take a simple arithmetic mean to form the chronology. Applying the transformation to the tree indices (rather than the chronology indices) has the advantage that the empirical distribution is accurately defined by such a large sample (e.g., for the Yamal TRW chronology developed here, 96,599 individual values are used rather than 2770). A limitation of this approach is that it is more appropriate for stationary data, and anomalous growth values associated with significant non-stationarities (e.g. the influence of major volcanic cooling events or of an "anomalous" warming trend) will, after transformation, be constrained in their magnitude by being drawn from the same overall normal distribution. Despite this caveat, the transformation offers an improved representation over the untransformed data, because the degree of positive skew of the latter is large and this results in an underestimate of the magnitude of low growth anomalies relative to high growth anomalies.

4.5. Estimation of chronology confidence

There are various ways to estimate the statistical confidence of a tree-ring chronology (Fritts, 1976 Chapter 6; Cook et al., 2002, 2013). We use the standard error of the mean chronology (i.e. the standard deviation of the individual tree index values available in each year divided by the square root of the number of samples) to indicate chronology confidence. To obtain confidence intervals for different timescales, we filter the tree indices prior to calculating the standard error. A commonly used measure of chronology confidence is the Expressed Population Signal (EPS; Wigley et al., 1984; Briffa and Jones, 1990) but this is normally determined mostly by the strength of the high-frequency common signal since it depends on the mean correlation between tree indices often calculated using a relatively short moving window or a longer, but still relatively short, common overlap period (Briffa and Cook, 2008; Jones et al., 2009). In SM6 we describe a modification to the EPS calculation (Melvin and Briffa, 2013b) which takes better account of the long-timescale as well as the short-timescale noise in a chronology and hence is a much-improved indicator of chronology confidence where low-frequency variance is retained. A related approach is to randomly sample with replacement from the available tree index series and construct bootstrap estimates of the chronology, though here we limit our use of bootstrapping to an analysis of data from the "Greater Urals" region (SM9).

5. Yamal Peninsula chronologies

The collection of tree-core samples and cross sections of sub-fossil tree stems began in this region in 1982 and has continued since, with additional impetus provided by the European Union funded ADVANCE-10K project in the late 1990s and continues with support from the Russian Foundation for Basic Research. These efforts produced a continuous 4000-year long larch (*Larix sibirica* Ledeb.) chronology whose year-to-year variability was shown to be associated with changes in June and July temperatures (Hantemirov and Shiyatov, 2002). The sample data that spanned the Common Era comprised some 265 sub-fossil samples and 17 of the longest-lived living-tree samples drawn from 5 sites in the region, originally selected by the authors to aid the preservation of medium-frequency variance in the chronology. This chronology was produced using a standardisation technique known as the "corridor" method (Shiyatov, 1986). While this method can retain medium-term climate information (on timescales typically ranging from inter-annual to century) it did not preserve longer (i.e. multi-centennial) growth variability in the chronology.

The same TRW measurement data (as used by Hantemirov and Shiyatov, 2002), were subsequently reprocessed, using the basic one-curve RCS approach, in an effort to produce a 2000-year chronology that better represented longer (centennial and above) timescales of tree growth and climate change. These analyses revealed evidence of prolonged periods of anomalous regional growth rate and inferred summer temperature anomalies: relatively cool summers in the late 2nd, and in the early 4th and 7th centuries and most dramatically, evidence for prolonged cool conditions spanning most of the 15th, 16th and 17th centuries. Periods of relative warmth were revealed in the 3rd, late 4th and late 8th/early 9th centuries as well as in the medieval period (late 10th/early 11th centuries) and on average across most of the 20th century. Evidence of higher, late 20th-century growth was, however, based on very few samples (as shown in Fig. 7 of Hantemirov and Shiyatov, 2002, see also SM5 Figs. PY28 and PY29).

A subsequent evaluation of the robustness of the earlier RCS chronologies (Briffa and Melvin, 2009) used additional Yamal data that were available in 2000 CE, including improved modern sample replication (70 living trees instead of the sub-sample of 17 trees). Much the same picture of past summer-temperature variations was reconstructed: including the evidence of relative warmth in medieval times and the 20th century (including years after 1980). None of these Yamal investigations supported the contention that medieval summers were significantly warmer or cooler than those of the 20th century in this region (see further discussion in Section 1.5 of CRU 2010: http://www.cce-review.org/evidence/Climatic_Research_Unit.pdf).

5.1. A re-analysis of Yamal data

The data set of larch ring-width measurement series used in the new analysis presented here contains 473 dated sub-fossil series and 160 living-tree samples from the Yamal region. This is a large increase over the 252 sub-fossil and 17 living-trees used in Briffa et al. (2008). The evidence of absolute dating fidelity for all these samples, based on routine dendrochronological cross-dating (inter-comparison of the inter-annual variability in multiple series) is available via SM2 part YT1. These data were separated into 12 groups which were treated as separate "site" collections for analysis purposes, the largest group being the sub-fossil material (see SM2 Table YT2 for details of the subdivision).

To demonstrate the patterns of common tree-growth between sub-groups at multi-decadal and shorter timescales, separate sub-group chronologies were created using 100-year high-pass-filter standardisation for each site. Fig. 2 illustrates the correspondence in tree-ring width changes for the different groups across the Yamal region over the last 400 years, with no further filtering (Fig. 2a) and after they were 10-year low-pass filtered (Fig. 2b). The chronology representing the sub-fossil data available in this relatively recent time window (navy blue) shows good correspondence with the living-tree chronologies at multi-decadal timescales. The correspondence in growth variability between all groups is very strong with little between-group scatter in the smoothed curves, especially when the tree replication of a group is relatively high. Taken together with the strong high-frequency chronology correspondence (reflected in the high cross-dating statistics – see SM2) this is clear evidence of a strongly coherent regional TRW response to a common tree-growth influence in this region at these (inter-annual to multi-decadal) timescales.

However, accurately representing the longer time-scale (centennial and above) growth variations requires a circumspect exploration of the use of the RCS approach. To do this we processed the sub-fossil and living-tree groups, both separately and together, using different implementations of the "signal-free" RCS to examine how best to extract the long-timescale growth signal from these data (see SM1 for more details of the general approach and of the specific implementation of signal-free RCS used here). Where systematic differences exist in growth rates between sites, even under similar climates, the use of a single RCS curve (using the data from all sites) can lead to a biased chronology at times when the number of samples from one site overwhelms those from the others. This can also be a particular problem within a site if commonly used sampling procedures favour coring of relatively large living trees. This is not unusual practise because often the intention is to acquire the longest record possible which tends to exclude young, relatively slow-growing individuals and potentially biases the recent part of the chronology, producing anomalously large values i.e. the so called 'modern-sample bias' effect (Melvin, 2004; Briffa and Melvin, 2011). The 2004 and 2005 sampling at Yamal did include trees with different diameter, but the observation that long-lived trees are often slower-grown will still lead us to expect some degree of modern sample bias. Because there are sufficient samples, it was possible to sub-divide the sample data into relatively fast and relatively slow growing classes (and to use two or more RCS curves rather than one) to explore whether the resulting sub-chronologies show parallel changes over time or whether there is a tendency for fast-growing trees to dominate the overall chronology variance at any time, particularly during the recent period.

Here we explore the sensitivity of the chronology (and its variance) by using one-curve, two-curve (and in SM2 Figs. YT13 and YT14, three-curve) RCS to standardise the overall Yamal data set (i.e. data from all 12 groups are pooled together before calculating the RCS curves). Fig. 2c and d show the average of the standardised indices for each sub-group after the (combined modern and sub-fossil) Yamal data set is processed using one-curve RCS and two-curve RCS respectively. The associated RCS curves and additional information are provided as Supplementary material (SM2 Fig. YT09). Comparing the alternative indications of low-frequency patterns of changing tree-growth (Fig. 2c and d) shows partial agreement but the spread between individual sub-group curves is less when two-curve RCS is used. The relatively high recent values at the CCC, POR and YAD sites after 1980 in the one-curve RCS implementation are reduced when two-curve RCS is used, because many samples from these sites fall in the class of relatively fast growing trees. Data from one site (Khadyta River, KHAD) appear anomalous with respect to the majority of site curves and after further investigation these data were not used in the subsequent analysis (see SM2 part YT3).

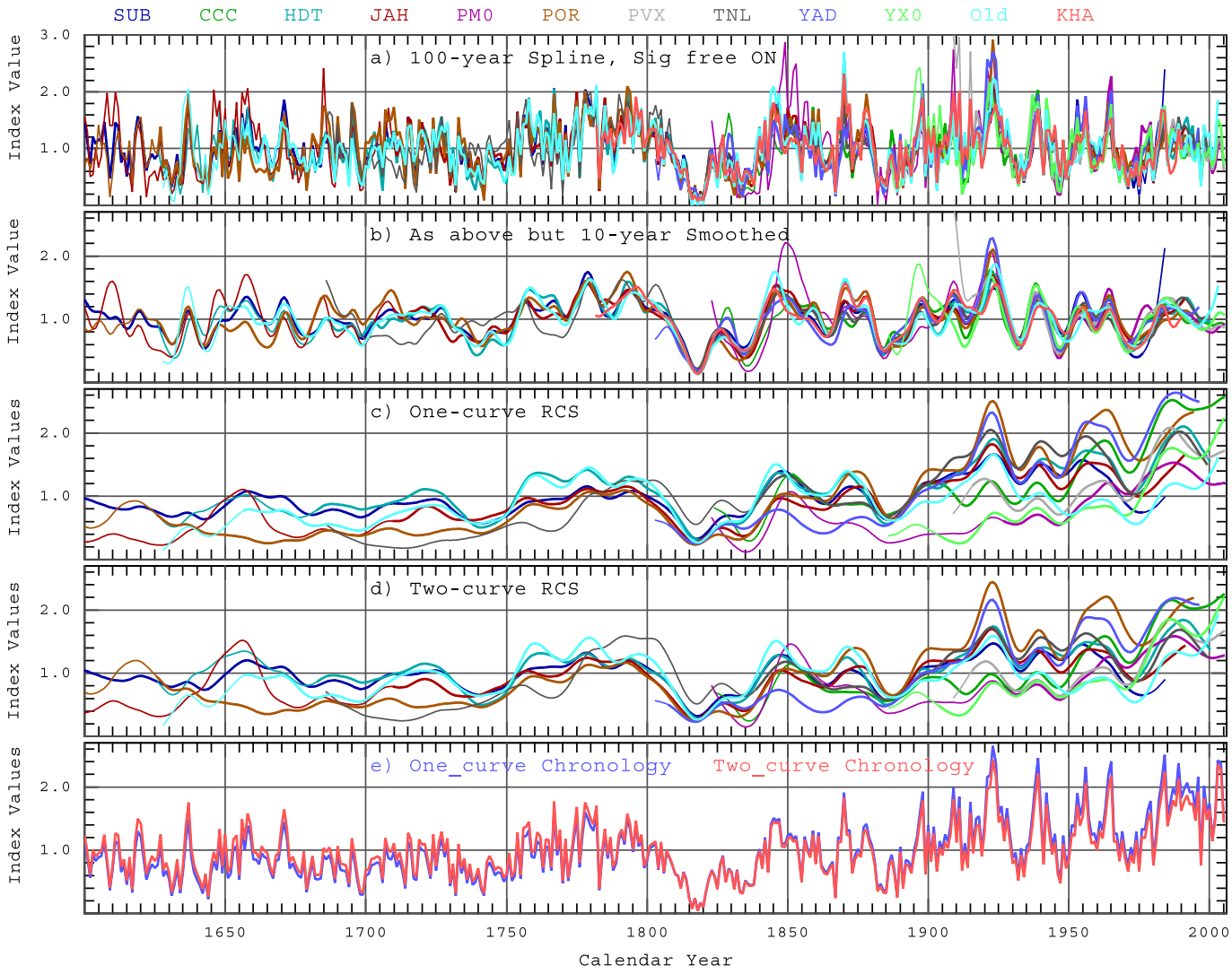

Fig. 2. Demonstration of the consistency of the medium to high frequency signal in chronologies created from sub-groups of Yamal data (see SM2 Table YT1 for site details). In (a) and (b), the raw data were standardised using a 100-year high-pass spline, signal-free standardisation and are shown averaged for each site (a) and then additionally smoothed with a low-pass 10-year spline to highlight the medium-frequency variability (b). These site data (excluding the data from Khadytla; see SM3 part YT3 for discussion) were also pooled into one data set and standardised using either one-curve SF RCS (c) or two-curve SF RCS (d). The tree indices for each sub-group were then averaged together to produce separate sub-chronologies and smoothed with a 20-year spline for display. The recent spread of the site chronologies is smaller for two-curve RCS than for one-curve RCS. The two versions (either one-curve or two-curve SF RCS) of the Yamal chronology are shown in (e) without smoothing for the period after 1600. The difference between one and two-curve RCS can be seen as a small change in slope over the period of living trees. In all panels, thinner lines indicate where the sample count <4.

The most recent 400 years of the alternative (one or two-curve RCS) chronologies are shown superimposed in Fig. 2e. Both mean chronologies show essentially the same pattern of low-frequency variability during the last 2000 years except for the modern period. The recent data for the one-curve RCS implementation indicate slightly higher late-20th-century tree-growth values than the two-curve RCS. This suggests some “modern sample bias”, associated with the influence of high-growth-rate trees or trees from relatively high-growth sites in recent decades.

The separate chronologies for the slower and faster growing classes, each standardised with their associated RCS curve (Fig. 3a), express very similar growth changes over time (Fig. 3b). Thus we have two “independent” chronologies showing essentially the same result. In contrast, if the tree indices from each class are standardised with a single RCS curve, but then averaged into a separate chronology for each class, the different growth rates are clearly reflected in the difference in the mean level of each chronology, though the decadal-to-centennial variability is clearly still similar (Fig. 3c).

The pattern of variability over time of each overall chronology (Fig. 4) is the net balance in changing growth, exhibited by relatively fast and relatively slow growing Yamal trees. In the case where one-curve RCS is used, the full chronology is the count-weighted average of the two curves shown in Fig. 3c, while the two-curve RCS chronology is the count-weighted average of the curves shown in Fig. 3b. For most of the chronology span, the numbers of relatively fast and slow growing trees is not greatly different (Fig. 3d), and both overall chronologies (Fig. 4) show generally similar patterns of growth changes through time, particularly where sample replication is not low.

Between 1600 and 1850 the number of slower-growing trees exceeds that of faster-growing trees, and after 1850 the number of faster-growing trees is greater (Fig. 3d). For the one-curve RCS, the chronology mean will lie nearer the blue line in Fig. 3c between 1600 and 1850, and it will be nearer to the red line in Fig. 3c after 1850. If the greater number of faster-growing trees after 1850 is a true reflection of the control of climate on tree growth rates then this will produce a genuine indication of recent increasing tree

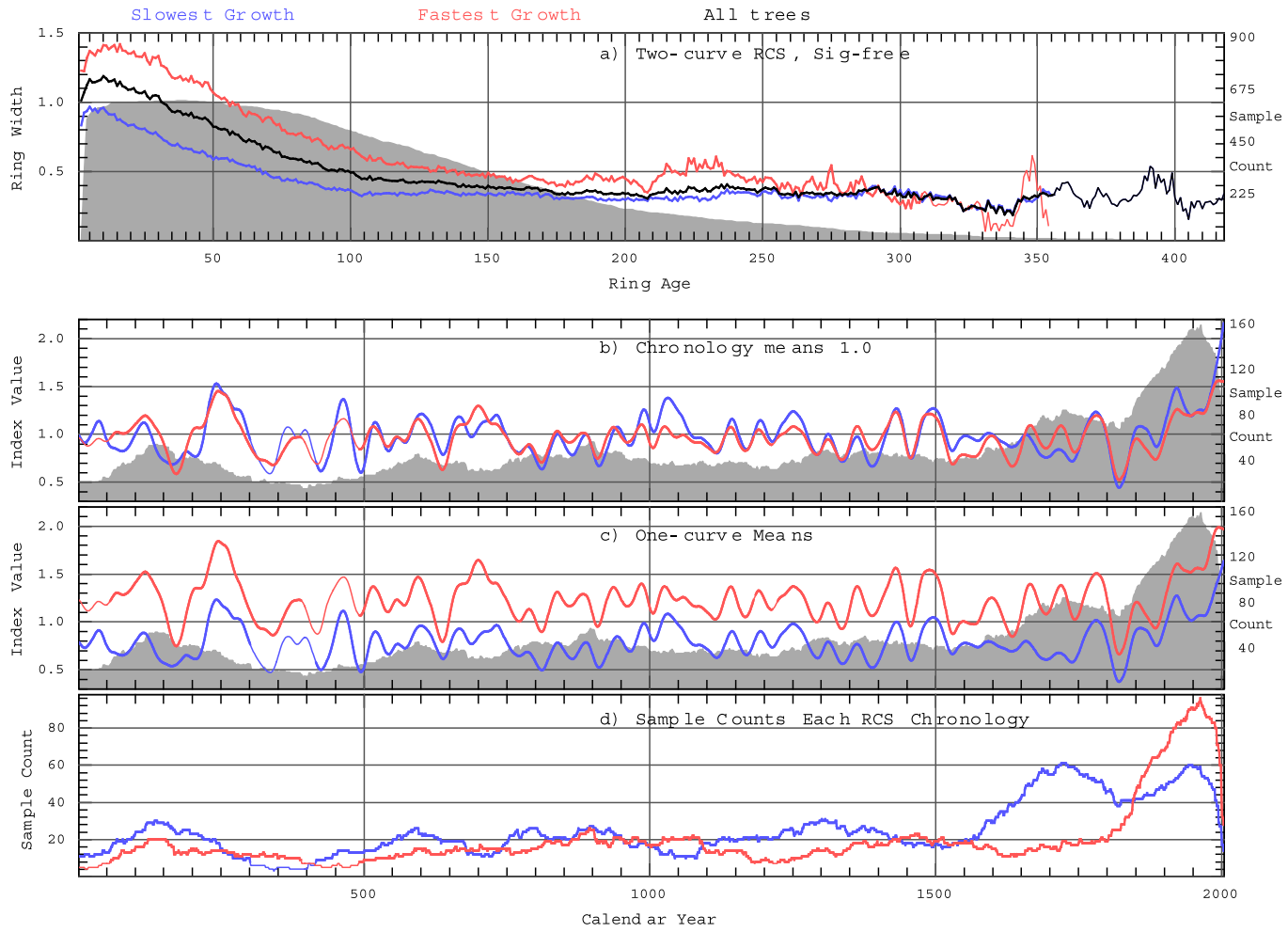

Fig. 3. The Yamal data (excluding Khadytla) were combined into one data set (yml-all.raw), with total sample counts shown as grey shading (right-hand scale) as a function of ring age (a) and calendar year (b and c). The data were either standardised using one-curve SF RCS or were split into two equal groups according to growth rate and each group was standardised with its own RCS curve (two-curve SF RCS). The single RCS curve (black) and two sub-RCS curves (faster growth rate, red; slower growth rate, blue) are shown in (a). The sub-chronologies obtained from the two growth-rate groups each have a mean of approximately 1.0 and these independent chronologies generally express very similar growth changes over time (b). Means of the same two groups of trees (fast and slow growing) but created by averaging the tree-index series produced using one-curve RCS reflect the relative overall difference in growth rates of the two groups of trees as well as the coherent variability in growth rates over time (c). Chronologies were smoothed with a 50-year spline for display purposes and sample counts of relatively fast or slow growing trees are shown in (d). In all panels, sections with sample counts below 8, shown by thin lines, are less reliable. (For interpretation of the references to colour in this figure legend, the reader is referred to the web version of this article.)

growth. However, in the period covered by living trees, some of the changes in the distributions of faster and slower growing trees are likely to be the consequence of "modern sample bias" (see earlier discussion) and not a result of changing climate. So using only one RCS curve could produce an exaggerated indication of recent tree growth. If the chronology is created using two-curve RCS and the means of these chronologies are approximately the same (as in Fig. 3b) changes in the relative distribution of faster and slower growing trees will have much less effect on the chronology. There is a possibility, however, that some long-timescale variability could be lost (see earlier discussion).

Fig. 4 compares the one-curve (black) and two-curve (blue) signal-free RCS Yamal chronologies over the last circa 2500 years. The third (red) line shows the two-RCS curve chronology formed by first transforming the tree indices so that their probability density function (PDF) corresponds to a normal (i.e. Gaussian) distribution. This is a novel development in RCS processing but is considered justified because the indices are fractional deviations (i.e. expressed as a ratio of the expected growth curve value) and without this transformation their PDF is positively skewed (see Section 4.4 and SM5 part PY2). Within the context of the chronology error (discussed later), there is little difference between the alternative chronologies, except that the two-curve RCS chronology (and its "normal" equivalent) shows a slightly lowered growth level from 1920 onwards. We consider it likely that the difference between the one-curve and two-curve RCS chronologies is attributable to the effect of "modern sample bias" in the one-curve RCS chronology and we choose to adopt the "conservative" two-curve RCS chronology to correct this problem.

Transforming the tree-index values to have a normal distribution reduces the amplitude of high chronology values and amplifies some strongly negative chronology values (e.g. 1815–1820; Fig. 4c). The high-growth years in the modern period are reduced relative to the untransformed two-curve RCS chronology (Fig. 4c), lowering the average 20th century chronology (Fig. 4b), as well as lowering some earlier periods with high chronology values (especially around 450 BCE, but also around 250 CE).

6. Polar Urals chronologies

In the Polar Urals region there are sub-fossil and modern-site sample collections both of which include ring-width and wood

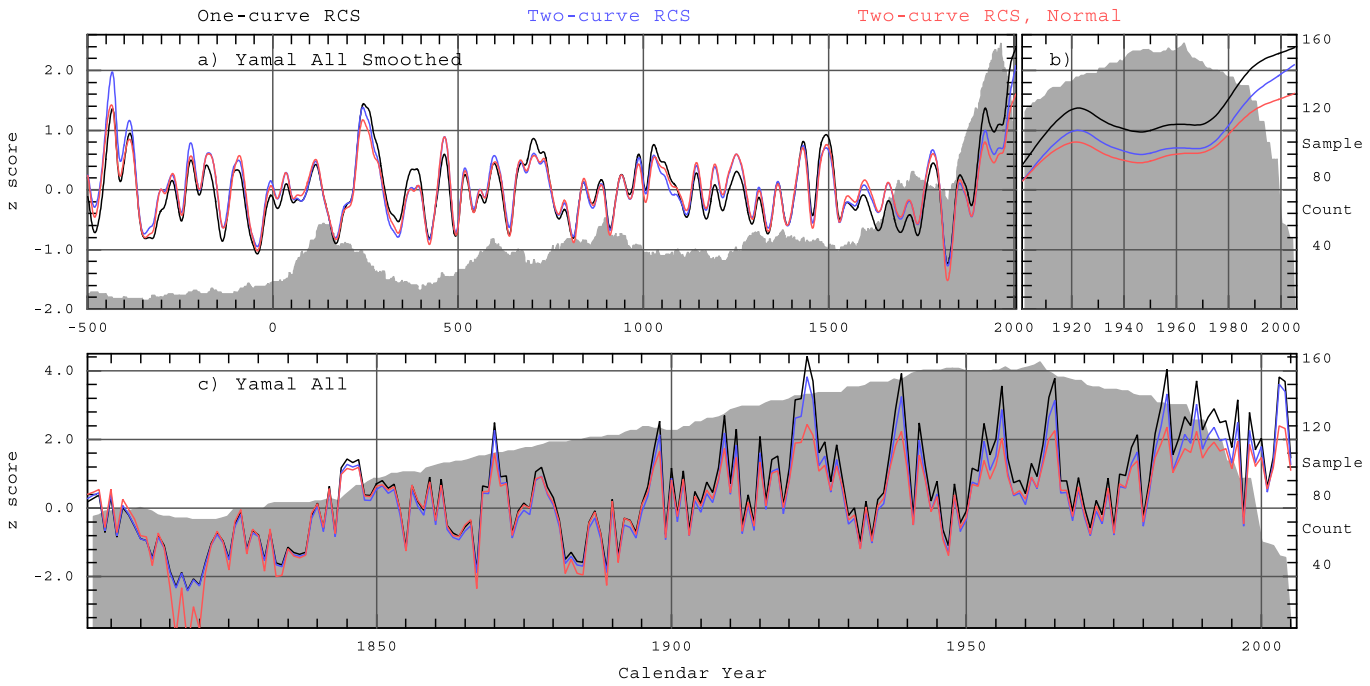

Fig. 4. The Yamal data (yml-all.raw) were used to create three different chronologies, standardised using one-curve RCS (black), two-curve RCS (blue) and two-curve RCS with tree indices transformed to have a normal distribution (red). Chronologies shown from 500 BCE in (a) and from 1900 (b) have been smoothed with a 50-year spline for display purposes, with (b) expressed on an expanded horizontal scale. The annually-resolved chronologies from 1800 to 2005 are shown without smoothing in (c). The three chronologies have been rescaled to have a mean of zero and unit standard deviation over the period 1 to 1600 CE. Tree counts are shown by grey shading and right-hand scales. (For interpretation of the references to colour in this figure legend, the reader is referred to the web version of this article.)

density data. The Institute of Plant and Animal Ecology, Ekaterinburg have been monitoring and recording the growth of near tree-line trees on the eastern slopes of the Urals, in the Sob river basin, for some 50 years (Shiyatov, 1962, 1986, 1995; see also SM3 part PU1), and a 1000-year ring-width chronology running up to 1969 provided the basis of an early (TRW only) summer (June and July) temperature reconstruction for the area (Shiyatov, 1986; Graybill and Shiyatov, 1992). This reconstruction, like the Yamal chronology of Hantemirov and Shiyatov (2002) described above, was based on "corridor" standardisation (Shiyatov, 1986). This provided clear evidence of relative short-term cold periods (1610–40, 1810–20, and 1850–80) and relative warmth in 1790–1809 and notably 1950–1969. While there is evidence that the corridor standardisation of these data was superior to other earlier processing methods (e.g. based on taking residuals from negative exponential curves fit to individual series of tree measurements), it did not retain information about relative tree-growth changes occurring over long (greater than centennial) periods (e.g. see Fig. 9c in Briffa et al., 1996).

In 1991, living trees of both larch and spruce (*Picea obovata*) were sampled by Fritz Schweingruber (The Swiss Federal Institute for Forest, Snow and Landscape Research (WSL), Birmensdorf, Switzerland) specifically for densitometric analysis (e.g. Polge, 1966; Schweingruber et al., 1978; Schweingruber and Briffa, 1996). Selected sub-fossil larch samples were also analysed to provide both MXD and TRW data. Continuous larch TRW and MXD chronologies spanning the period 914 to 1990 CE were constructed initially based on the Hugershoff curve-fitting standardisation (Bräker, 1981; Schweingruber and Briffa, 1996), that again removes low-frequency variations.

These MXD data were later processed using a single (linear) RCS curve to produce a chronology which, along with a spline-standardised TRW chronology from the same samples, was used to produce a summer temperature reconstruction that showed more long-timescale variability than had previously been reconstructed from these sample data (Briffa et al., 1995). The strength of the relationship between observed summer (May to September) temperature variability and that of the MXD ensured that this reconstruction was overwhelmingly controlled by changes in the MXD chronology, with the TRW data exerting only a small influence (see SM5 Fig. PY29b). However, the MXD and TRW chronologies were poorly replicated in parts and their reliability was particularly poor prior to about 1100 CE (see Fig. 1c in Briffa et al., 1995). Comparison of the MXD-dominated Polar Urals temperature reconstruction (Briffa et al., 1995) with the RCS-processed TRW data from the adjacent Yamal Peninsular region (see Fig. 1f in Briffa, 2000) showed inconsistencies, particularly in the decades around 1000 CE, when the Polar Urals MXD suggested relatively cool summers but the Yamal RCS (and even the Polar Urals TRW, when standardised using RCS; Fig. 7 of Briffa et al. (1996)) indicated relatively warmer summer conditions at that time.

In June 1999, specifically with the intention of improving the Polar Urals sample replication, additional sub-fossil larch samples were supplied (SM3 part PU3) and processed in Birmensdorf to provide new MXD data and associated TRW measurements. These data (provided as Polurula in Supplementary material) were archived in September 2000 in the International Tree-Ring Data Bank http://www.ncdc.noaa.gov/paleo/treering.html. The TRW measurements from these samples, along with the TRW measurements arising out of the earlier densitometric measurement of the Polar Urals samples described above, were included as part of a large-scale TRW-only analysis of circum-polar tree-growth and implied hemispheric temperature changes through the last millennium described in Esper et al. (2002, see also Cook et al., 2004). These authors used RCS to standardise all of these data, expressing the TRW measurements as anomalies from one of two RCS curves (curvilinear or linear) constructed by averaging data from 14 sites and multiple species across the hemisphere (see also Briffa and Melvin, 2011).

Esper et al. (2002) did not present the Polar Urals data explicitly in the form of a regional chronology. Nor did they advocate their use as an optimum regional representation of tree-growth or temperature changes for the Polar Urals (or Yamalia) region. However, other authors (e.g. Hegerl et al., 2007; Ljungqvist, 2010; Shi et al., 2012) have subsequently used the "Polar Urals" component chronology extracted from the Esper et al. (2002) groups of regional RCS indices, in all cases combining RCS TRW indices from larch and spruce, in preference to earlier published RCS-based chronologies or temperature inferences that are both longer and better replicated, e.g. (Briffa, 2000; Briffa et al., 2008). The Esper et al. RCS Polar Urals TRW data indicate considerably higher tree growth and implied warmth, particularly in the periods 950 to 1100 and 1400 to 1600 CE, than can be inferred from the other Yamalia RCS series.

Here we describe new analyses that include the "original" (i.e. the Pou_la data used by Briffa et al., 1995, 1996) and later "updated" (i.e. the Polurula data used by Esper et al., 2002) Polar Urals larch data. These are supplemented with additional and more recent TRW and MXD measurements, from living larch trees, that allow the earlier TRW and MXD data to be extended to 2006 (see SM3 Table PU1). The evidence of dating fidelity and the strong interannual timescale coherence in all of the TRW and MXD data is demonstrated by the cross-dating summaries provided as supplementary information (SM3 part PU2).

6.1. Processing the Polar Urals TRW data

For exploratory analysis of longer-timescale variability, the existing (at the time of Esper et al., 2002) Polar Urals data are separated into three sub-groups: original sub-fossil data (Pou_la); "updated" sub-fossil (Polurula); and living-tree sample data ("modern"). Fig. 5a compares the medium-frequency (10–100 years) variance in these separate data sets. Taking into account the poor replication in the Polurula chronology after about 1700, there is very good agreement between all of the curves.

However, when all of the TRW data are standardised together with a single RCS curve and the separate sub-group chronologies compared, a discrepancy in the low-frequency variability between the original (Pou_la) and "update" (Polurula) TRW data is clearly evident (Fig. 5b). Closer examination of the details of the sample material reveals that the Polurula samples comprise a relatively large proportion of root-collar wood. The root-collar (or root crown) refers to the lower section of the tree bole (stem), generally near the soil surface, where the bole meets the upper parts of individual roots and is frequently associated with an expansion in the stem diameter at this point. It would be expected that ring width dimensions in such root-collar samples would be systematically larger than equivalent rings measured higher in the boles of the same trees. It is also the case that average ring dimensions in the root-collar vary greatly when measured at different positions around the circumference, according to the positions of the major roots.

Fig. 5d–e illustrate how much of the discrepancy in the low-frequency curves for the Pou_la and Polurula data sets is due to the relatively large number of root-collar derived measurements in the latter, by separately identifying the mean and low-frequency variations in the different types of sample (red and purple lines indicate root-collar samples). The root-collar samples have more variable (and generally larger) ring dimensions than regular stem samples, here sampled at varying levels above ground depending on the height of remnant tree boles. Assuming a single (RCS) expectation of ring width as a function of tree age when standardising the bole and root-collar measurements together leads to systematically larger indices for the root-collar data in the 11th and 15th centuries (compare Figs. 5b, c and 6a) and smaller indices for the bole samples. The meta-data relating to the "original" Pou_la sub-fossil sample collection show that this also contains three root-collar samples (out of a total of 50 sub-fossil samples). However, the "update" Polurula data used by Esper et al. (2002) include 18 root-collar samples (out of a total of 32 sub-fossil samples) (see SM3 Figs. PU05 to PU08 and associated text for further details).

The Polurula samples were apparently collected and processed with the intention of improving the poor replication of samples in the early section of the Pou_la chronology (see tree counts in SM3 part PU3). Fig. 5f also shows the dramatic changes in the standard deviation of the full (amalgamated stem and root-collar data) chronology during periods that are dominated by the inclusion (higher standard deviation) of root-collar data. As these root collar samples appear highly variable in terms of cross-sectional dimensions, rather than being generally symmetric, it is not appropriate simply to process them with a separate (root-collar) RCS curve and it was considered necessary to remove these samples from the Polar Urals TRW RCS chronology despite the already low chronology replication (see SM4 description and Fig. PC02).

A consolidated Polar Urals TRW (Polar.raw) dataset was assembled by combining the original and updated sub-fossil data (excluding the data from root-collar samples) together with the original modern data and additional modern data (see SM3 Table PU1). These additional data raise the maximum modern sample replication from 18 to 56 and extend the series through to 2006. There are now at least 20 samples from 1650 onwards. Data from the Russ001 site (21 cores ending in 1968) used previously by Graybill and Shiyatov (1989) were not used because neither pith-offset estimates nor densitometric measurements were available for those samples, limiting the accuracy of RCS standardisation and the comparison of the TRW and MXD Polar Urals chronologies. Nevertheless, we show in SM3 (Figs. PU11 to PU13) that the Russ001 site data are fully consistent with the data used in the main paper.

Fig. 6 presents three TRW chronologies obtained from this consolidated and updated Polar Urals dataset, using one- or two-curve SF RCS, and a third case where the two-curve RCS tree indices are transformed to have a normal distribution prior to averaging to form the chronology. The use of two-curve, rather than one-curve, RCS and the subsequent transformation of tree indices has much less effect on the modern part of the chronology than was the case for the Yamal TRW data (Fig. 4), with the modern effects mostly limited to the very recent (post 1990) section of the chronology (Fig. 6c). As with the Yamal chronology, the preferred two-curve RCS chronology has less of a growth depression in the 17th and 18th centuries, and the relatively high growth in the early decades of the 11th century is similarly reduced, though we stress the very low replication (and large uncertainty) in the Polar Urals chronology at this time.

The influence of the expanded network of living-tree samples is apparent by comparing Fig. 6 with Fig. 5c (the latter only included the modern data used in previous studies). The additional modern data have strengthened the chronology trend from 1890 to present. The more recently collected site data show faster growth rates over the same period than the single-site data used in the original analysis even when the TRW data are processed using two-curve RCS (see SM3 Fig. PU13). The new smoothed chronology values are higher than all earlier periods in the 1100+ year record. This comparison should be treated with caution, however, due to the potential end-effects of the smoothing spline, and a more appropriate assessment of the periods with strongest (and weakest) growth in each of the chronologies is presented later.

6.2. Processing the Polar Urals MXD data

Densitometric data are available for all of the Polar Urals samples used in the previous section, including the various sub-fossil

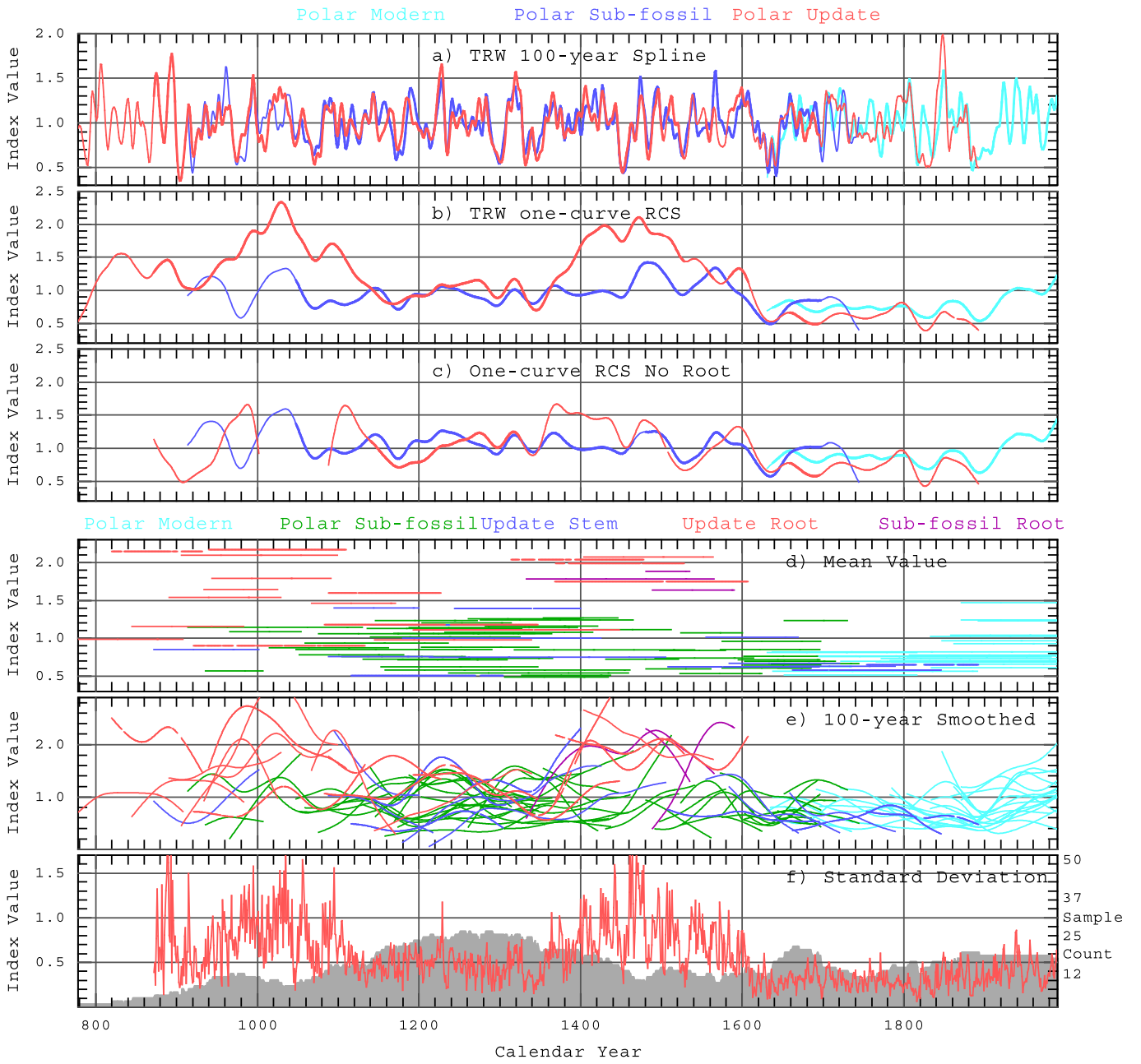

Fig. 5. Chronologies constructed using TRW data from the Polar Urals (Pou_la_mod.raw, Pou_la_sub.raw and Polurula.raw), shown separately in (a–c) for averages of the "original" sub-fossil (blue), the "update" sub-fossil (red) and the modern (cyan) tree indices. The chronologies are constructed here using: (a) all data and 100-year high-pass spline, signal-free standardisation; (b) all data and one-curve, SF RCS; and (c) all data excluding the root-collar samples and one-curve, SF RCS. The chronologies are smoothed with (a) a 10-year or (b–c) a 50-year spline for display, with thin lines used where <4 trees are available (the sub-set chronology sample counts are shown in SM3 Fig. PU04). The individual-tree mean index values are shown as horizontal lines spanning the years with rings in d) and the similarly plotted 100-year smoothed tree-index series are shown in e), coloured to identify: "update" root-collar samples (red), "update" stem samples (blue), "original" stem samples (green), "original" root-collar samples (purple), and modern, living-tree samples (cyan). The sample counts (grey shading) and standard deviations (red) of all individual tree indices (including root-collar samples) are shown for each year in (f). (For interpretation of the references to colour in this figure legend, the reader is referred to the web version of this article.)

collections and modern sites that extend the record through to 2006. The ".mxd" sites listed in Table PU2 of SM3 are used here. As is the case for the Polar Urals TRW data, there are far fewer Polar Urals MXD data than Yamal TRW, especially during the sub-fossil period. The root-collar bias in the MXD data is considerably smaller than in the TRW data (compare Fig. 5 with the SM3 Fig. PU09), and so, while the root-collar samples were omitted from the Polar Urals TRW chronology because attempts to "correct" for their bias were not considered feasible, a correction of the smaller MXD bias was attempted and allowed us to maintain the MXD root-collar series.

It has recently been shown how MXD data measured at different times or in different laboratories may be systematically different (Helama et al., 2008, 2012; Melvin et al., 2013). As the Polar Urals MXD data are made up of different collections, processed between 1991 and 2007, we explored whether such systematic differences might exist between them. We compared the mean signal-free index series (these are time series for each sample after standardisation to remove the effect of tree age and after removal of the common chronology variability) and found it necessary to apply adjustments to the MXD data to make the different MXD data

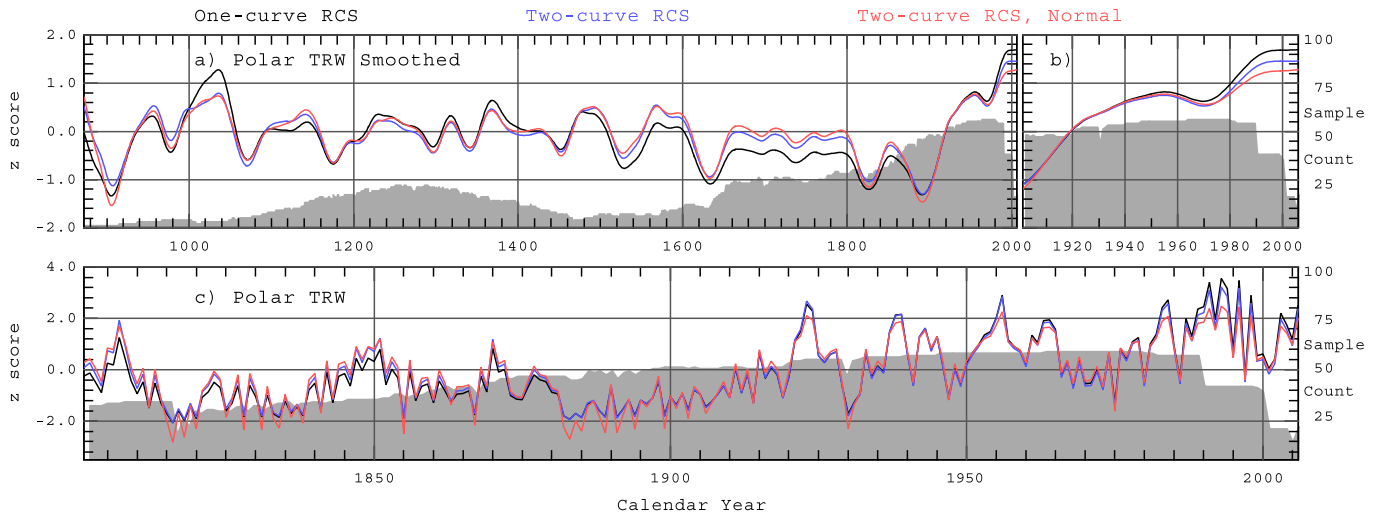

Fig. 6. As Fig. 4 except that TRW data from the Polar Urals are used (excluding root-collar samples and including additional samples ending in 2001 and 2006; polar.raw). The three chronologies have been rescaled here to have a mean of zero and unit standard deviation over the 900 to 1600 CE period before smoothing.

collections compatible with each other (extensive details are provided in SM4).

Fig. 7 shows chronologies produced using the currently available MXD for the Polar Urals: these include the adjusted Polar Urals MXD data sets; Pou_la_modadj.mxd, Pou_la_stem.mxd, Polurulaxadj.mxd and Purlaaxadj.mxd used to produce Fig. 7a and b and polarxs.mxd used for Fig. 7c–e (see SM4). Fig. 7a shows the separate Polar Urals MXD sub-groups after standardisation with a 100-year spline and 10-year low-pass filtering for display. Where the sample replication is at least four, there is close correspondence at these medium-frequency timescales between all series. Fig. 7b shows the separate Polar Urals MXD sub-chronologies after the pooled sites were standardised using one-curve, signal-free RCS and 50-year low-pass filtering for display. The consistency between the low-frequency signals in the MXD sub-chronologies is notably poorer in Fig. 7b than in 7a, similar to the comparison in the Polar Urals TRW (Fig. 5a and c). This is likely due to a weaker low-frequency common signal, possibly related to low replication. This strongly reinforces the rationale for comparing and consolidating the TRW and MXD data within this Yamalia area in an attempt to increase the signal to noise ratio of these data.

As with the TRW data, we also apply one- and two-curve, signal-free RCS standardisation to the consolidated Polar Urals MXD data, with a third chronology obtained by transforming the two-curve RCS tree indices to have a normal distribution (Fig. 7c–e). These three options all provide similar MXD growth histories. As with the Yamal and Polar Urals TRW (Figs. 4a and 6a), the two-curve RCS reduces the level of relatively high-growth in the 20th century but also reduces the extent of relatively low growth in the 17th and 18th centuries. The adjustment of the MXD data sets has reduced the between-site effects of "modern sample bias" and the two-curve RCS reduces the within-site effects of "modern sample bias". It is a moot point as to how much of the amplitude of climate-induced tree growth changes over the last 500 years is lost. As for the Polar Urals TRW, there may be some. The low-frequency component of the MXD chronology is the least reliable but in the temperature reconstructions described in Section 11 we use only the high- to medium-frequency variance in these MXD data. With this caveat, and for consistency, we adopt the two-curve implementation of RCS for the MXD data. The transformation of the tree indices to follow a normal distribution makes only a small difference here, because the untransformed MXD tree indices are less (here negatively) skewed than the TRW indices.

7. Comparing TRW and MXD chronologies

Fig. 8 shows the three updated and consistently processed chronologies, Yamal TRW, Polar Urals TRW (omitting root-collar samples), and Polar Urals MXD (after adjustment of the raw data to counter possible processing biases), all constructed using two-curve RCS with tree-indices transformed to have a normal distribution prior to averaging. Fig. 9 provides a comparison of the low-frequency evidence for changing tree-growth provided by the three datasets, after they have been smoothed with a low-pass 50-year spline. Note that each chronology, plotted as annual values with 50-year smoothing superimposed, is shown in SM5 (Figs. PY24 to PY27). Taking Figs. 8 and 9 together, the general agreement between all three chronologies at high, medium and in large part also at low frequency is apparent. For example the correlation between the Yamal and Polar Urals TRW chronologies is 0.82 for timescales less than 15 years, 0.78 between 15 and 100 years, and 0.69 at when they are smoothed with a 100-year spline (see also SM5 Figs. PY30 and PY31). Periods with similar growth anomalies are apparent in all three chronologies but there are also periods of disagreement evident, especially before 1100 and between 1440 and 1570, but the low replication of the Polar Urals series at these times should be borne in mind.

The Yamal TRW chronology is shown in two sections, 500 BCE to 871 CE (Figure 9a) and 872 CE to 2005 CE (Fig. 9b), the latter matching the overlap period with the two Polar Urals chronologies (Fig. 9c and d). In Fig. 9 two versions of each chronology are shown: the one-curve and two-curve versions of the signal-free RCS (three-curve RCS results are also shown in SM5 Fig. PY21). In assessing Fig. 9, attention should be paid to the large differences in replication between series and through time and associated differences in the low-frequency chronology confidence intervals (here expressed as ±2 S.E. of the mean chronology created from 50-year smoothed tree indices and plotted about zero) (see also SM6).

Chronologies created using one-curve and two-curve RCS are generally very similar. Other than in the last four centuries the use of a second RCS curve removes very little long timescale variance. The main difference arising from the use of a second RCS curve is a reduction in the slope of the last four centuries in all the chronologies. The Polar Urals TRW also has reduced values in the 13th and 14th centuries. It is likely that the poorer replication of the Polar Urals data is having an effect (i.e. through higher noise levels) and

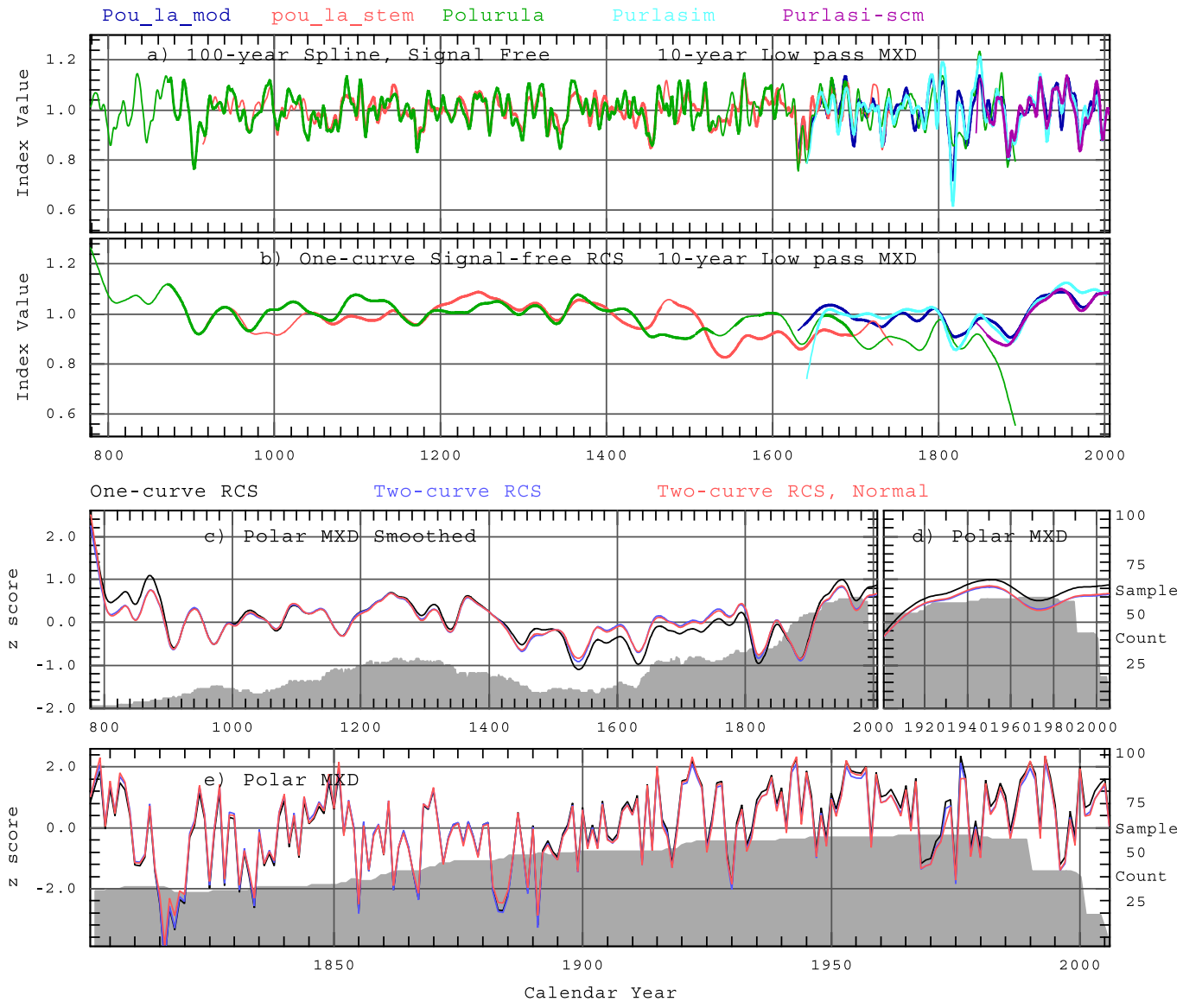

Fig. 7. Chronologies constructed using "adjusted" MXD data from the Polar Urals (Pou_la_modadj.mxd, Pou_la_stem.mxd, Polurulaxadj.mxd and Purlaaxadj.mxd used in (a) and (b) and polarxs.mxd used for (c), (d) and (e)). Chronologies of the means of tree indices are shown separately in (a) and (b) for the averages of the "original" sub-fossil (red), the "update" sub-fossil (green), the original modern data (blue), and the additional modern data collections (cyan and purple). The chronologies are constructed using all data and: (a) 100-year high-pass spline, SF standardisation; and (b) one-curve, SF RCS. Chronologies were smoothed with a 10-year spline and thin lines are used where tree counts are <4. Three further chronologies constructed from the pooled, adjusted Polar Ural MXD data (polarxs.mxd) and standardised using one-curve SF RCS (black), two-curve RCS (blue), and two-curve RCS with tree indices transformed to have a normal distribution (red). Chronologies shown in (c) and (d) were smoothed with a 50-year spline for display purposes, with (d) showing the period since 1900 on an expanded horizontal scale. The chronologies from 1800 to 2006 are shown without smoothing in (e). The three chronologies have been rescaled to have a mean of zero and unit standard deviation over the period 900 to 1600 CE before smoothing. Tree counts are shown by grey shading. (For interpretation of the references to colour in this figure legend, the reader is referred to the web version of this article.)

that this effect is greater in TRW than MXD because the TRW series has a larger proportion of variance manifest at long timescale than does MXD. Again we stress that applying two-curve RCS potentially leads to some loss of low-frequency trends, particularly in the shorter sub-chronologies derived from living-tree data only. However, the living-tree proportions of the long reconstructions are very prone to the effects of modern sample bias that, if not removed, will exaggerate any positive (climate-forced) trend over the past 100–400 years.

Though there is some variation in precise timing, comparison of the medium to low-frequency variance in these chronologies, reveals a number of common periods of low or high growth. Common low growth periods are apparent in the first two decades of the 10th century, the two decades centred on 1170; around 1290–1305; 1330–50; 1445–70; 1520–30 and 1815–20 and the 1880s. The last of these is not so prominent in the Yamal data as in the Polar Urals, which results in the 1820s being arguably the most prominent decadal timescale, low-growth anomaly, especially when considering sample replication and general chronology confidence. Except for a brief high period in the late 18th century, all chronologies indicate generally protracted low growth from 1610 through to 1840. The growth in both Polar Urals series remains low to about 1910. The Polar Urals MXD chronology, despite exhibiting good decadal agreement with the other series, shows generally low growth also throughout the 15th and 16th centuries that is not in agreement with the low-frequency variability of the other series. Because of the large error in the Polar MXD (and TRW) at this time, we consider the low-frequency information in

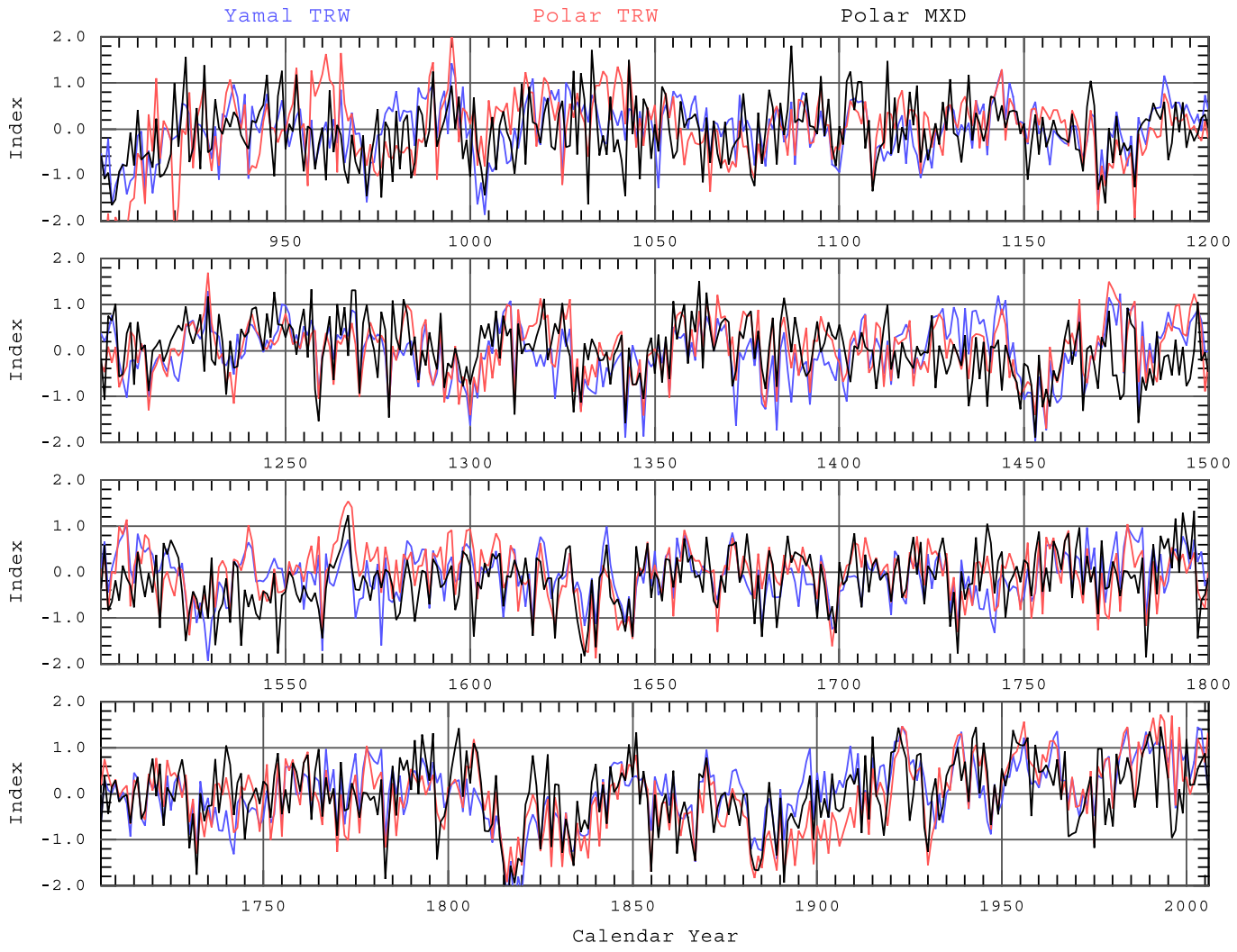

Fig. 8. Comparison of the new chronologies from this work plotted from 900 CE, created using two-curve SF RCS with tree indices transformed to have a normal distribution, for each of the Yamal TRW (blue), Polar Urals TRW (red) and Polar Urals MXD (black) data sets. Note the 100-year overlap in timescales of the bottom two panels. (For interpretation of the references to colour in this figure legend, the reader is referred to the web version of this article.)

the MXD chronology to be likely more unreliable during this period.

As for common high-growth periods, 1020–1040, the decade centred on 1140 and 1240–1270 are identifiable. The period 1470–1510 is notably high in both TRW series but below the long-term mean in the MXD series, a discrepancy that might be ascribed to the long-timescale uncertainty in the latter series mentioned above. The 1420–1440 period also shows significantly higher growth in the Yamal series, but not in either of the other, less reliable, chronologies.

The Yamal TRW chronology extends back more than 1000 years before the Polar Urals chronologies. The earlier Yamal chronology shows high-growth periods between circa 450 to 425 BCE and 400 to 370 BCE but the chronology is poorly replicated (between 6 and 8 trees) at these times and less reliable in comparison with the better replicated later periods. However, there is another prominent period of high tree growth shown in the 3rd century CE (see Fig. 9a and e). Following two low growth years in 220 and 221, the chronology values increase rapidly to a very high level by 225 and, but for a few individual low growth years, this is maintained until a rapid decrease in 268. The high growth during this circa 40-year period is equivalent to the highest level of growth in the late 20th century (see Fig. 9g and Table 1). The replication in this 3rd century period is generally good (between 25 and 33 trees) and the standard error range low. Also each of the relatively fast or slow growing sub-chronologies (whether based on one-, two- or three-curve RCS) shows this period as anomalous (see Fig. 3 and SM5 Fig. PY11), demonstrating that this is likely a reliable and notable indication of previous high tree growth rate in this region.

The most prominent period of relatively high growth, and one expressed in both of the TRW and the MXD chronologies, occurs after about 1920 (see Table 1; Fig. 9g). From a period of low growth, in the 1880s, all series increase, maintaining a level of generally high growth throughout the last 80 years in comparison to the overall chronology mean. Allowing for the various chronology uncertainties, the recent high growth level is possibly the highest of any equivalent multi-decadal period in the last millennium (though note that the standard error is not negligible). Note again that the high growth in the Polar Urals TRW in the early decades of the 11th century is less reliable as a consequence of the very low replication (less than four samples).

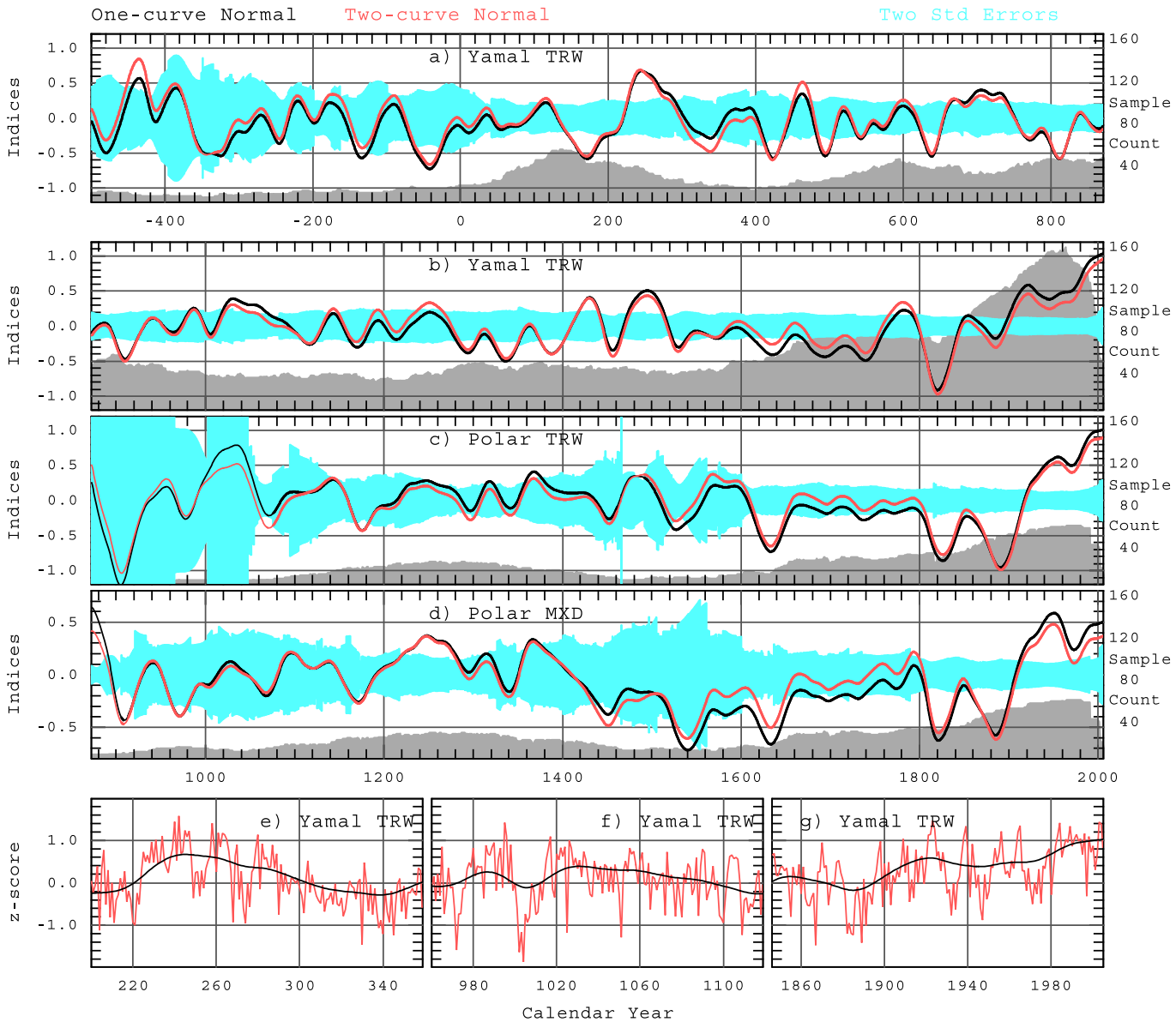

Fig. 9. Comparison of chronologies created using one-curve (black) and two-curve (red) SF RCS with tree-indices transformed to have a normal distribution for (a) the early and (b) the later sections of the Yamal TRW data and the Polar Urals TRW (c) and Polar Urals MXD (d) data sets. Chronologies have been smoothed with a 50-year spline for display purposes and thin lines show where tree counts are <6. For the preferred (red) curve, ±2 S.E. of the mean are shown for 50-year smoothed data as cyan shading. Where <4 samples are available S.E. is not calculated and the cyan shading spans the full *y*-axis range. Annual and smoothed values of the "preferred" two-curve RCS chronology are shown for three sub-periods (200–350 (e), 970–1120 (f), and 1840–2005 CE (g)). Sample counts are shown by grey shading. Note the different horizontal scales in (a). (For interpretation of the references to colour in this figure legend, the reader is referred to the web version of this article.)

8. The evolution of the Yamal RCS TRW chronology

Fig. 10 summarises the evolution of the common-era Yamal TRW chronology from the use of simple one-curve RCS (Briffa and Cook, 2008; Briffa et al., 2008) applied to the comparatively small data set compiled by Hantemirov and Shiyatov (2002); to the later similar RCS processing of a larger dataset, supplemented with additional measurements running up to 1996 (Briffa and Melvin, 2009); and finally to the current series based on two-curve, signal-free RCS applied to a larger measurement data set containing more sub-fossil and additional modern data running up to 2005 (see also SM5 Figs. PY30 and PY31). We argue here that the use of the two-curve, rather than one-curve, RCS mitigates the likely influence of "modern sample bias", as discussed by Melvin (2004), Briffa and Melvin (2011) and Melvin et al. (2013) and demonstrated here by the differences between the one-curve and two-curve RCS versions being manifest mainly in the recent centuries of all chronologies.

For the first time in the development of the Yamal chronology, the tree indices are transformed to have a normal distribution, prior to their averaging to form the final chronology (see Section 4.4; SM5; Melvin and Briffa, 2013a for more details). Without this transformation, the PDFs of the constituent TRW indices and of the chronologies themselves are positively skewed (and the MXD slightly negatively skewed; see SM5 part PY2 for more discussion). Fig. 10 also demonstrates what effect our recent processing (i.e. signal-free application of two-curve RCS and the transformation of tree indices to have a normal distribution before averaging) would have had on the earlier published versions of the Yamal TRW chronology. The one-curve RCS chronologies (which are similar to the original published curves – see SM5 Fig. PY28) are shown in black; the effect of two-curve RCS processing is shown in blue; and

Table 1
Common Era periods with the highest and lowest mean values for the Yamal TRW chronology. The chronology was created using two-curve, SF RCS with tree indices transformed to have a normal distribution. Means of chronology values and inter-annual standard deviations of those chronology values are shown for 25-year, 50-year and 100-year non-overlapping periods.

Positive anomalies				Negative anomalies			
Rank	Period	Mean	S.D.	Rank	Period	Mean	S.D.
25-year periods							
1	1981–2005	0.89	0.39	1	1814–1838	−1.05	0.64
2	224–248	0.75	0.36	2	796–820	−0.69	0.59
3	454–478	0.56	0.27	3	158–182	−0.64	0.44
4	1423–1447	0.51	0.44	4	405–429	−0.64	0.53
5	1905–1929	0.50	0.50	5	483–507	−0.61	0.46
50-year periods							
1	1955–2004	0.61	0.53	1	1795–1844	−0.56	0.73
2	223–272	0.58	0.52	2	770–819	−0.45	0.62
3	1470–1519	0.38	0.48	3	134–183	−0.41	0.54
4	1896–1945	0.35	0.55	4	307–356	−0.40	0.39
5	691–740	0.34	0.52	5	404–453	−0.36	0.56
100-year periods							
1	1906–2005	0.47	0.56	1	1797–1896	−0.34	0.69
2	205–304	0.29	0.61	2	125–224	−0.28	0.53
3	654–753	0.25	0.51	3	330–429	−0.28	0.61
4	1423–1522	0.18	0.67	4	1293–1392	−0.25	0.64
5	1184–1283	0.17	0.47	5	770–869	−0.24	0.61

the two-curve RCS with transformation to a normal distribution in red. All chronologies have been normalised (by subtraction of the mean and division by the standard deviation) over their length up to 1600 CE. All curves are shown for 2000 years, with 50-year smoothing in the upper panels and as individual yearly values since 1800 CE in the lower panels. This allows the recent end-effect of the smoothing to be judged. The grey shading indicates the changing sample replication.

The major growth anomalies are remarkably consistent in all versions of the chronologies. The differences in the series are only really apparent after about 1600 and in general the effect of applying two-curve RCS is less than the effect of the tree-index transformation, except in the case of some years around the 1990s in the most recent, best replicated, chronology. All chronologies show relatively low growth in the 19th century followed by a strong growth increase in the early 20th century and another increase to a higher mean level after 1980. If the data are shown only as smoothed data the very recent increase in tree growth in the last decade of the upper two panels is overly accentuated. Smoothing through to the ends of a series always introduces some form of end-effect bias (whether a cubic spline (Peters and Cook, 1981) is used as in the current paper or a Gaussian weighted filter as in Fig. 1f of Briffa (2000)) which is why it is important to consider the annual values shown in Fig. 10d–f. The recent section of the chronology shown in Fig. 10a and d is made from TRW data from three sites: YAD, POR and JAH (see SM2 Table YT2 and Fig. YT03); when using one-curve RCS recent growth rates of trees at POR and YAD are slightly above those at JAH (see Fig. 2c and Briffa and Melvin, 2009).

In Fig. 10d (Briffa, 2000; Briffa et al., 2008) the last two chronology years (1995 and 1996) are made up of data from only 5 trees, all from the YAD site. The previous 6 years (1989–1994) had data from 10 trees, from both the POR and YAD sites. The combination of low sample numbers and the fact that these samples originated from relatively old trees with a large recent growth increase implies a slight positive bias in the post-1990 part of the original Briffa (2000) and Briffa et al. (2008) chronologies.

The chronologies shown in Fig. 10b and e contained data from 20 trees up to 1994 and 10 trees in 1995 and 1996, though again the 1990s are represented by data from only the POR and YAD sites (these used the "Yamal-All" data described in Briffa and Melvin (2009) which include data up to 1990 from the KHAD site, but data from this site are not used in the final chronology presented here as stated earlier (and see SM2 part YT3)). Briffa and Melvin (2009) stated "*The post-1990 values in the new Yamal_All chronology are based only on data from the POR and YAD sites, and so are likely somewhat biased by the greater increase in recent tree growth rates observed there, …*". Comparing the chronologies built from the earlier datasets (Fig. 10a and d) with those built from the data used in the 2009 version (Fig. 10b and e), shows that the recent bias noted above is less than that in the earlier series.

The current Yamal chronology contains post-1990 data from a wider and hence likely more-representative range of sample sites than in earlier Yamal chronologies and has data that run through to 2005 (see SM2 Fig. YT3). In this new chronology the post-1985 increase in tree growth levels seen in the smoothed version of the previous series is less prominent. Except for low growth in 1997 and 2001 (see Fig. 10f), a consistently high level of tree growth is clearly maintained post 1980, as was also apparent in the previous RCS versions of the Yamal chronology and which is now seen for the first time, in the context of the last 2000 years, to be maintained through to the end of the new chronology in 2005.

The influence on the modern end of the Yamal TRW chronology of transforming tree indices to have a normal distribution is greatest for the earlier, smaller dataset (Fig. 10a and d). This transformation reduces highest growth values in all three chronologies (because the data are positively skewed prior to applying the transformation), but by a bigger margin for the earlier dataset. This is partly because the extreme chronology values are simply larger in that case (in terms of the number of standard deviations above the mean) and lie further into the positive tail that the transformation suppresses. However, a further consideration is that the transformation is applied to all of the tree indices (pooled together) prior to their averaging to produce a chronology. Two periods with similarly high chronology values, but with one period arising from all tree indices showing similarly high growth and the other arising from a mixture of slightly raised growth-rate and extremely large growth-rate trees, could be affected to different degrees by the transformation, with the latter period being more strongly reduced and perhaps representative of the recent period of the earlier dataset.

To the extent that this index transformation removes positive skew, dampens the influence of very high growth-rate trees and, in this example at least, reduces the sensitivity of the chronology to the inclusion of additional data (i.e. the differences between the red curves in Fig. 10 are quite small), this approach appears very promising. We do, however, raise the caveats that (i) forcing the data to follow a normal distribution may not be appropriate, especially in a non-stationary climate; and (ii) the transformation of the extreme low and high values will always be subject to greater error because the tails of an empirically-determined distribution are never completely accurate. In this instance, many of the highest values occur during the most recent decades. The reduction of these values by the transformation is more uncertain and could be overdone because the transformed values do not depend on the absolute tree index values, but solely on their rank position (see Section 4.4 and SM5 part PY2).

9. Medieval versus recent tree-growth levels

In the context of this review, if one defines the "Medieval Warm Period" (MWP) very loosely, as one of prolonged high tree growth (and implied summer warmth), assumed to occur sometime between 800 and 1400 CE, neither the TRW or the MXD data, either as previously analysed or as reassessed here, support the conclusion that the MWP is strongly manifest in Yamalia. The exception to this

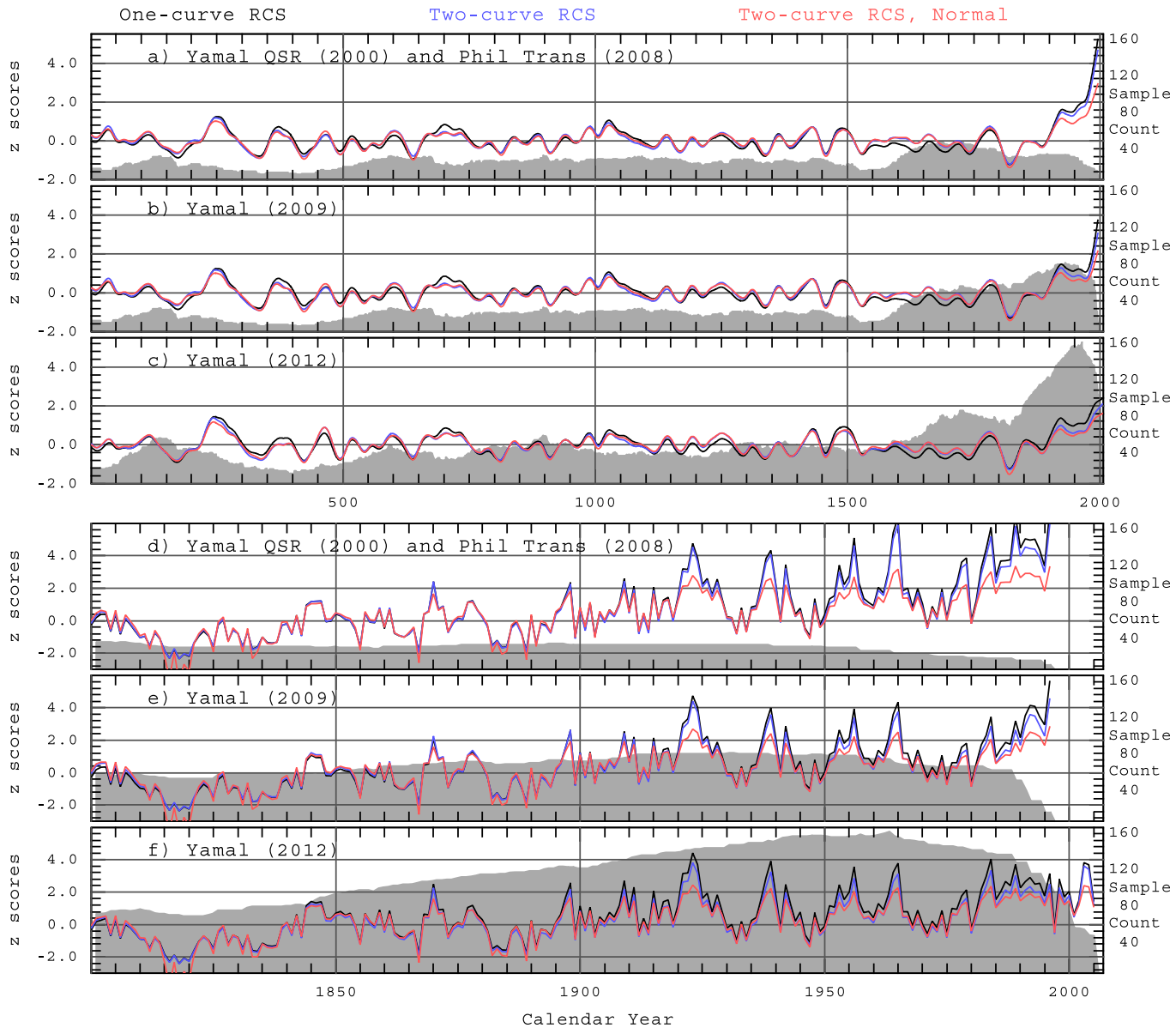

Fig. 10. The TRW measurement data sets used in Briffa (2000) and Briffa et al. (2008) (a), in Briffa and Melvin (2009) (b), and in the analysis described here (c), were each processed using one-curve SF RCS (black), two-curve SF RCS (blue) and two-curve SF RCS with tree-indices transformed to have a normal distribution (red). All chronologies were normalised (subtract mean and divide by standard deviation) over their length up to 1600. The CE portions of the chronologies are shown in (a) to (c) with 50-year smoothing and annual values for the last two centuries are shown in panels (d) to (f). Grey shading shows sample counts. (For interpretation of the references to colour in this figure legend, the reader is referred to the web version of this article.)

statement is the RCS-processed Polar Urals TRW data produced in Esper et al. (2002) and Cook et al. (2004). The reanalysis of these data here show that the apparent evidence for high tree growth in medieval times in the Polar Urals region (circa 980–1040) was exaggerated due to inclusion of root-collar wood samples. Of the three chronologies described here, the new Yamal TRW chronology provides the most reliable indication of long-timescale tree-growth changes in the region. This shows relatively high growth in the medieval time range, in 975–1001 and 1015–1060 but of lower magnitude than shown in Esper et al. (2002) Polar Urals data. Growth is also high in 1220–1270 (Figs. 9 and 10 and SM5 Fig. PY25), but the magnitude of the anomalies considered on a 50-year timescale at these times is not as great as for other high-growth periods: in the early 3rd and 15th centuries. Hence, while there is evidence of positive growth anomalies for multiple decades either side of circa 1000 CE, there is no strong evidence that "medieval" tree growth was notably high in Yamalia. High growth at this time in the reprocessed Polar Urals TRW data (see Figs. 6a, 8 and 9c) is based on very few samples and the associated statistical uncertainty (c.f. Fig. 9c) is correspondingly high. None of the statistically-reliable medieval-period multi-decadal growth anomalies shown in the TRW or MXD chronologies reach the magnitude of the most recent levels of growth, circa post 1920, whether considered on a 25, 50 or 100 year scale (see Fig. 9f and Table 1).

We note earlier work on tree-elevation changes on Rai-Iz Massiv, Polar Urals (Shiyatov, 1993) involving a survey of tree remnants extending over an elevational range from 280 to 340 m.a.s.l. during the period 850 to 1990 CE. This remains one of the most detailed studies of tree-line position and composition over time undertaken

to date. This work showed an early phase of relatively high larch germination at approximately 1100–1250, a notable phase of tree death at 1300–1350 and a complete absence of germination along the whole elevational transect from 1650 to 1900. The strong phase of tree germination at high elevation at the start of the twelfth century revealed in Shiyatov (1993) implies a distinct warming at that time. While some high growth-rate intervals are evident in our chronologies during the 1100–1250 period (Fig. 9), they are neither continuous nor notably higher than earlier or later intervals e.g. in the 11th and 15th centuries. It should also be noted that while the study area was virtually devoid of living trees at the start of the 20th century, it is now covered in larch forest (Shiyatov, 2009).

A comparison of selected long warm-season temperature reconstructions that retain low-frequency variability shows how the timing of major anomalies, including in medieval time, revealed in the Yamalia region are not geographically synchronous even with those shown in other parts of Eurasia. The apparent magnitude and precise timing of any warm anomaly depends, of course, on the reconstruction method (including the period over which data are calibrated (Esper et al., 2005)) and the degree of smoothing used to represent the chronology (Osborn and Briffa, 2004). Büntgen et al. (2005) show medieval warmth in the western Austrian Alps manifest prior to 1000 CE. Maximum medieval warmth at the Taimyr tree line (circa 71°N and 100°E) appears to span less than 100 years (between 950 and 1040 CE) and to be at least as warm as in recent decades (Naurzbaev et al., 2002; Briffa et al., 2008). In northern Scandinavia, some work also shows summer warmth that was likely close to the level of recent warmth but during the period 900–1100 CE (Buntgen et al., 2011; Melvin et al., 2013). However, Esper et al. (2012) identify a longer (circa 700–1250 CE) medieval period in north Scandinavia, the early part of which (circa 710–780 CE) is warmer than the 20th century mean. Helama et al. (2009) show the period of medieval warmth to be shorter in northern Finland (~850–1150 CE) and clearly cooler than recent values. Amalgamated multi-proxy tree-ring data from Norway, Finland, Sweden and western Russia (McCarroll et al., 2013) show altogether less clearly defined medieval warmth in the context of their overall chronology. So while all of these records, when averaged together, provide a general indication of circa medieval warm summers, it is advisable to be somewhat circumspect as to its precise magnitude and duration when considering the larger region. The same conclusions will arise when characterising the nature of widely perceived climate anomalies in other periods (such as the so-called Roman Warm Period) or wider geographic averages.

10. A new 'Yamalia' TRW chronology

The high coherence in the inter-annual and multi-decadal timescale variability between the Yamal and Polar Urals TRW data demonstrate the existence of a strong common growth forcing at these frequencies. The correspondence in long-timescale (centennial and longer) variability is not as good, but the poorer replication (and low-frequency chronology confidence) in the Polar Urals samples, at least before the 18th century, points to the Yamal chronology being the more reliable representation of long-timescale tree growth in this region. Nevertheless, there are still many common features between the chronologies as have been described earlier.

In order to incorporate all of the available TRW data for the Yamal and Polar Urals we have also produced a new 'Yamalia' chronology, as the count-weighted average of tree index series generated in producing the two-curve (with tree index transformation) Polar Urals TRW and equivalent Yamal chronologies. Given the higher replication of the Yamal data, the chronology is inherently weighted towards the Yamal series, but this is preferable to a simple unweighted average of the Yamal and Polar Urals TRW chronologies, which would give equal weight to the less-well replicated Polar Urals series. Over the period 900–2005 CE the correlation between Yamal and Yamalia TRW chronologies is 0.985. We present this Yamalia chronology (in SM5 Figs. PY24–25) running from −500 to 2005, but it should be noted that the data prior to 1 CE are not considered as reliable and the end date takes account of the fact that the 2006 data are from only one site in the Polar Urals. The earlier discussion about periods of high and low tree growth with respect to the CE portion of the Yamal chronology is equally valid in the case of the Yamalia TRW chronology. The subsequent part of this review examines the association between the Yamalia TRW series, the Polar Urals MXD and local meteorological data for this region and reviews a number of possible inferences about the history of past summer temperatures based on these TRW and MXD data.

11. Summer temperature inferences

The development of the tree-ring chronologies, including the selection and processing of the tree-ring measurements described in the earlier sections, was carried out in isolation of any comparison with the instrumental climate data. The aim here has been to maximise the common signal within the tree-ring chronologies and to minimise time-varying biases. This is distinct from maximizing the climate or temperature signal, though of course the expectation is that the common signal in this case will be a summer temperature signal because the samples were collected from near to the Arctic tree line. The instrumental temperature data are now used to identify the seasonal temperature signal in the ring-width and density chronologies, and to "calibrate" the chronologies to give an estimate of past temperature variability together with confidence intervals. We use the monthly temperature anomalies for the grid-box centred on 67.5°E, 67.5°N from the CRUTEM4v dataset (Jones et al., 2012). The early data, beginning in 1883, were observed at Salekhard, a weather station record used in earlier studies of tree-ring chronologies from this region (e.g. Graybill and Shiyatov, 1989; Briffa et al., 2008; Esper et al., 2009) with additional station data incorporated in more recent decades. A small number of missing observations in this grid-box series were infilled using scaled temperature anomalies from neighbouring grid boxes (see SM7). The separation of the temperature variability into frequency bands (<15 years, 15–100 years, and >100 years) is shown in SM7 Figs. CA02 to CA05.

Correlations for the full overlap period (1883–2005 or 2006) between the chronologies and temperature anomalies averaged across seasons of various lengths (see temperature correlations SM7 Fig. CA06) demonstrate a number of results relevant to the reconstruction of past temperatures. Inter-annual TRW variations correlate better with a shorter season (June–July, JJ, or even July only) than do MXD variations, which correlate most strongly with the June–August (JJA) season (though correlations with May and September are also at least 0.26). The maximum inter-annual correlation for the Yamal TRW chronology (0.69 against July) is greater than for the Polar Urals TRW chronology (0.63), and pooling the TRW data to form the Yamalia chronology makes little difference to the correlation, which remains weaker than the strongest correlation for the Polar Urals MXD chronology (0.82 against JJA). Correlations are stronger at interdecadal timescales: between JJ temperature and Yamal or Polar Urals TRW chronologies correlations are 0.78 or 0.73, respectively, while for Polar Urals MXD correlation with May–July temperature is 0.85 or 0.81 if June–August is considered instead.

These temperature correlations and the chronology confidence intervals presented earlier (Fig. 9; SM6) suggest the construction of

two distinct summer temperature reconstructions and the separate calibration of two frequency bands exhibiting variations on timescales less than 15 years ("high frequency") and between 15 and 100 years ("medium frequency"). The variations on timescales greater than 100 years ("low frequency") cannot be directly calibrated because there are insufficient degrees of freedom on this timescale during the 123-year instrumental temperature record; such a calibration would amount to scaling the series so that the trends had the same amplitude. Instead the scaling factor used to calibrate the medium-frequency data is also applied to the low-frequency data.

The first reconstruction ("Yamal-TRW") is based only on the Yamal TRW series, spanning the period −96 to 2005 when the replication is at least 10 samples, and is calibrated against June–July (JJ) temperature. This chronology provides the most reliable measure of tree-growth in the region over this time period, and we calibrate the high- and medium-frequency variations separately because TRW autocorrelation can suppress the response to short-term temperature excursions; lag-one autocorrelation for Yamal TRW is 0.53 and for JJ temperature is 0.22. The second reconstruction ("Yamalia-Combined") combines the interannual (high-frequency) variability of the Polar Urals MXD data with the longer-term (medium- and low-frequency) variability of the Yamalia TRW data (the latter is a chronology based on the combined Yamal and Polar Urals TRW series shown individually in Fig. 9 and SM5 Figs. PY24 and PY25). This combines the strengths of the two datasets: the clear response to short-term temperature changes in the MXD data and the better representation of the longer-term changes by the Yamalia TRW chronology because of its greater replication and comparatively lower error (Fig. 9). For this second reconstruction, we target both the JJ and JJA seasons (each a compromise between the optimal seasons for the MXD and TRW at the shorter and longer timescales), and limit the reconstruction to the period 914–2005 when the replication of the MXD series is at least six samples.

The temperature reconstructions are obtained by decomposing the tree-ring chronologies into three series (expressing variations on timescales less than 15 years, between 15 and 100 years, and greater than 100 years – see SM7 part CA2), simple scaling of each series, followed by summation to obtain the full reconstruction. The scaling factors can be determined by regression against the target instrumental temperature time-series. There are a number of possible regression approaches to consider (e.g. Esper et al., 2005; Burger et al., 2006; Moberg and Brattstrom, 2012). Regressing temperature onto the tree-ring chronology is a common approach in dendroclimatology, with the advantage that the reconstruction error during the calibration period is minimised, but the discrepancy between the series is implicitly assumed to be entirely due to errors in the temperature data and this erroneous assumption results in an underestimation of the scaling factor (b_t) and of the reconstructed temperature variations (e.g. von Storch et al., 2004). In contrast, regressing the chronology onto the temperature data and then using the inverse of the linear slope ($1/b_c$) to scale the tree-ring chronology leads to larger reconstructed temperature variations but also larger error estimates. Other approaches result in scaling factors that lie between these two extremes. For example, total least squares (also known as errors in variables) regression can be used where the ratio of proxy error to instrumental temperature error can be estimated (Hegerl et al., 2007; Mann et al., 2008) though further analysis and development of these methods is required, especially in the context of Bayesian approaches that allow prior information from other sources to be incorporated (Tingley et al., 2012). Scaling the variance of the chronology to match the variance of the temperature data over the calibration period also yields a scaling factor (b_v) that lies between the chronology-on-temperature and temperature-on-chronology regressions. "Variance matching" is also a form of regression, being equal to the geometric mean of the simple linear regression slopes ($b_v = \sqrt{[b_t/b_c]}$) and also referred to as the "geometric mean functional relationship" or "line of organic correlation" (Barker et al., 1988).

The outcomes of these various approaches are much less sensitive to the choice of regression method when the chronology–temperature correlation is strong (the ratio of b_t to $1/b_c$ is equal to r^2), and in this work the correlations (Table 2) are mostly near to 0.8 so the choice is less critical. The variance matching approach is used here to scale the tree-ring chronologies to represent temperature variations, though we also compare the derived scaling factors with those obtained using chronology-on-temperature or temperature-on-chronology regression (Table 2). These scaling factors are estimated using the full overlap period between chronology and instrumental data, with the exclusion of years near to the end of the filtered series to reduce the influence of end effects (see SM8).

For both the Yamal-TRW and the Yamalia-Combined reconstructions, each medium-frequency TRW series can be calibrated against the band-pass (15–100 year) filtered summer temperature data. There are, however, rather few degrees of freedom in this band-pass series during the calibration period and this will be reflected in higher uncertainty in the calibration scaling factor. An alternative approach is also considered where the band-pass TRW series is calibrated over a much longer period (1600–2005) against the band-pass calibrated MXD series (see SM8 for further details). The resulting scaling factors are included in Table 2 for comparison. The reconstruction uncertainty ranges are estimated from a combination of time-varying chronology confidence intervals and a time-invariant "temperature representation uncertainty". This latter term is intended to express the error that would still arise even if the chronology itself were a perfect representation of regional tree growth, because tree-growth is not perfectly correlated with summer temperature. We estimate the amplitude of this so that, when combined with the chronology uncertainty, the total uncertainty is sufficient to capture the residuals between temperature and reconstruction at a particular timescale (the residuals are shown in SM8 Figs. ST02–ST06).

The magnitude of the chronology uncertainty relative to the total uncertainty for the Yamal-TRW reconstruction (Fig. 11) is small at high-frequencies and becomes larger as the timescale lengthens, until it represents almost all of the error at centennial timescales. Another way to express this is that, at the 100-year

Table 2
Calibration parameters for the Yamalia and Yamal summer temperature reconstructions.

Chronology	Band (yr)	Season	σ_T (°C)[a]	$r(T,C)$[b]	Scaling factor (°C)		
					T-on-*C*[c]	Var. match[c]	*C*-on-*T*[c]
Polar Urals MXD	<15	JJA	1.16	0.83	1.71	2.05	2.46
		JJ	1.40	0.77	1.92	2.48	3.20
Polar Urals MXD	15–100	JJA	0.43	0.86	1.31	1.51	1.75
		JJ	0.58	0.85	1.73	2.04	2.40
Polar Urals MXD	<100	JJA	1.31	0.82	1.62	1.96	2.38
		JJ	1.61	0.79	1.89	2.40	3.05
Yamalia TRW	15–100	JJA	0.43	0.75	1.14	(2.00) 1.51	2.01
		JJ	0.58	0.84	1.71	(2.45) 2.04	2.44
Yamal TRW	<15	JJ	1.39	0.58	2.05	3.54	6.11
Yamal TRW	15–100	JJ	0.58	0.82	1.70	2.07	2.51

[a] Standard deviation of filtered temperature.
[b] Correlation between filtered temperature and filtered chronology.
[c] Scaling factors applied to the chronology based on temperature-on-chronology (*T*-on-*C*), variance matching, and chronology-on-temperature (*C*-on-*T*) regression; for Yamalia TRW, alternative variance matching scaling factors are given in parentheses based on the calibration of these data against the calibrated Polar Urals MXD.

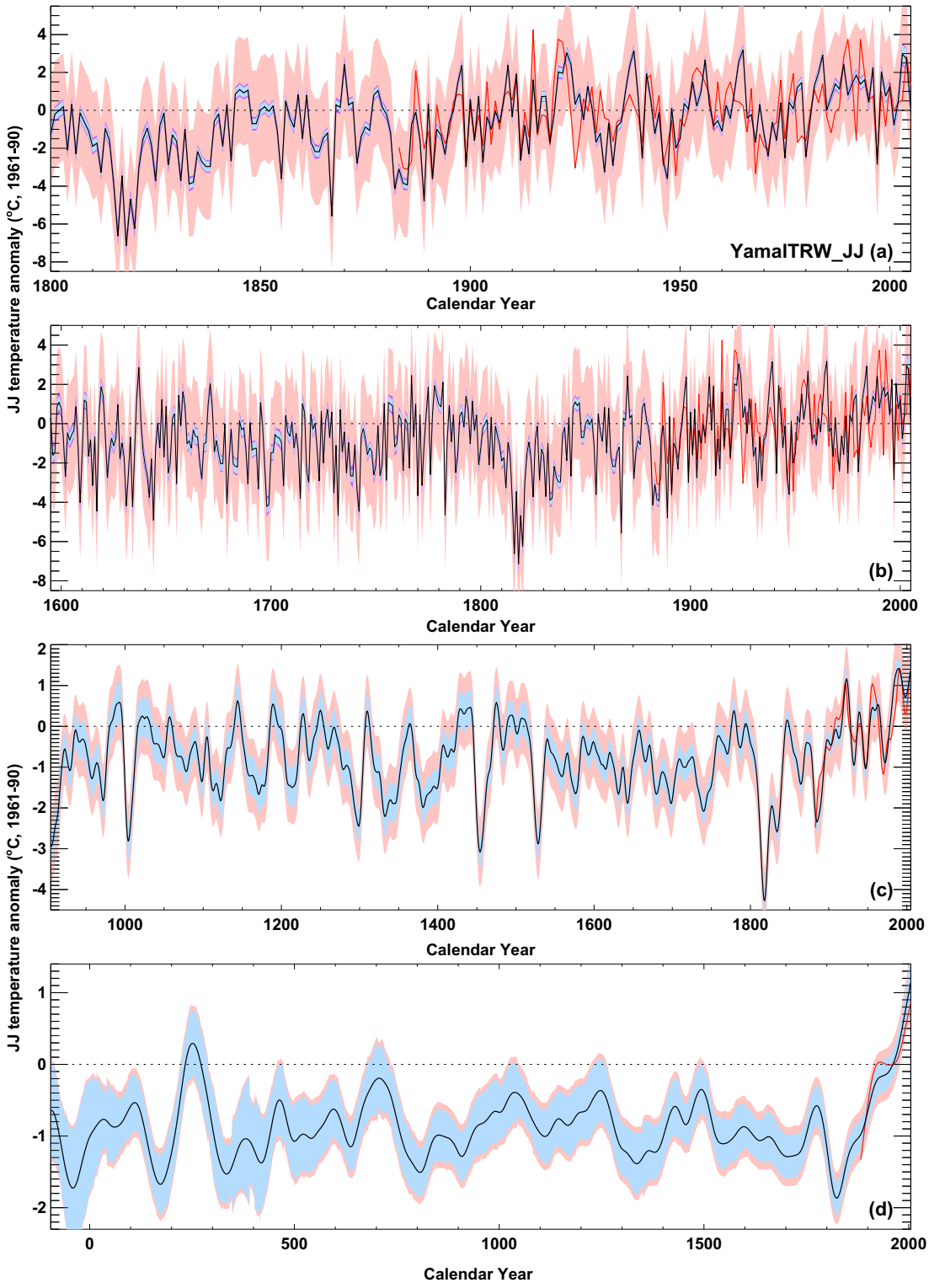

Fig. 11. The "Yamal-TRW" JJ temperature reconstruction (black line, °C anomalies from 1961 to 1990 mean) and its confidence interval (shading: pale blue for combined medium- and low-frequency chronology uncertainty; purple for high-frequency chronology uncertainty; pale red for "temperature representation" uncertainty), in comparison with the instrumental temperature (red line): unfiltered reconstruction for (a) 1800–2005 and (b) 1595–2005; (c) 15-year smoothed reconstruction for 905–2005; and (d) 100-year smoothed reconstruction plotted from 96 BCE onwards. Note that the smoothed values at the ends of the series are more uncertain due to the presence of end effects on the spline filters, especially for (d). (For interpretation of the references to colour in this figure legend, the reader is referred to the web version of this article.)

timescale (Fig. 11d), the chronology uncertainty of the Yamal TRW reconstruction is almost sufficient to explain the difference between the calibrated chronology and the temperature record, and implies only a small additional "temperature representation uncertainty". The total uncertainty for the unfiltered reconstruction (Fig. 11a and b) indicates that there are relatively few years when, considered individually, the estimated summer temperature was significantly cooler than the 1961–1990

reference level, and almost none when it was significantly warmer (with half of those few cases occurring after 1900). A very prominent exception to this is the 1815–1821 run of seven years with temperature estimates around 6 °C below the 1961–1990 mean, while a four-year run from 1882 to 1885 has estimated temperature anomalies of about −4 °C. Other examples are discussed later.

On timescales of 15 years and longer, the Yamal-TRW reconstruction uncertainty is much reduced because of the close fit between the calibrated chronology and the instrumental temperature (Fig. 11c; see also SM8 Fig. ST02). There are many extended periods where the temperature estimates are significantly cooler than the 1961–1990 mean, with strong cooling (~3 °C) inferred around 1000, 1450 and 1530, and the coolest period centred on the late 1810s. There are a number of relatively warm intervals, though for the period shown in Fig. 11c the only cases where the lower end of the uncertainty range exceeds the 1961–1990 reference level all occur after 1900. Two further such intervals (239–245 and 260–264), preceding the period shown in Fig. 11c, contribute to the warm interval inferred in the third century CE at the 100-year timescale (Fig. 11d). This is one of the few periods where the reconstructed temperatures do not lie clearly below the 1961–1990 reference. Although the central estimate for the temperature in this warm period centred around 250 CE is below that for the recent period, when we take into account the reconstruction uncertainties, the slight overestimation of the recent trend by the reconstruction, and the end effects that increase the uncertainty of the filtered series, it is not possible to be certain that recent warmth has exceeded the temperature of this earlier warm period. Taking the highest 50-year means of the unfiltered data (Table 1), there is no statistically significant difference between the reconstructed temperatures for 1955–2004 and 223–272 CE. This early warm period was, however, both preceded and followed by periods of low TRW and so the central estimates of the temperature reconstruction averaged over the warmest 100-year period near the 3rd century CE (205–304 CE) are about 0.4 °C cooler than the 1906–2005 mean. This is 1.2 times the estimated standard error of the difference (using the reconstruction uncertainties for the 100-year timescale). Since we *a priori* expected the modern period to be warm, a one-tailed test indicates that differences that arise by chance due to errors in the temperature reconstruction (rather than because the actual temperatures warmed) are smaller than this 87% of the time. It is likely, therefore, that summers during the last 100 years were warmer on average in this region of northwest Siberia than in any other century during the last 2000 years.

The Yamalia-Combined summer temperature reconstructions (Fig. 12) exhibit similar features to the Yamal-TRW reconstruction; this is to be expected for timescales longer than 15 years because much of the TRW data are common between these series, but at high-frequencies the data are less dependent (MXD versus TRW). The relative role of chronology uncertainty does not become as large at low frequencies (blue shading in Fig. 12d and e compared with 11d) because this uncertainty is smaller during the instrumental period (due to higher replication by the inclusion of the Polar Urals TRW into Yamalia) and yet the residuals are larger, thus implying a notably larger "temperature representation uncertainty". This effect is bigger when the target is JJA temperature (Fig. 12d), which is not optimal for the TRW data and thus the residuals are larger; it is less apparent when the target is JJ temperature (Fig. 12e). The Yamalia-Combined reconstructions also tend to slightly overestimate the warming trend relative to the instrumental temperature (we have made no attempt to fit the 100-year trend in the data; instead the reconstruction trend depends on the scaling factor obtained for the medium-frequency calibration). Note additionally that the final decades of the 100-year filtered series are much more uncertain than shown because of the end effects of the spline filtering.

The Yamal-TRW and Yamalia-Combined reconstructions are compared at a range of timescales and for different time periods in Fig. 13. The high-frequency variations show similar periods of inferred warming and cooling, but the estimated uncertainty range is smaller for the Yamalia-Combined reconstruction that utilizes the Polar Urals MXD data with its high-fidelity short-term signal. The amplitude of the cold intervals is slightly stronger in the Yamal-TRW reconstruction in most cases, with the stronger calibration scaling factor (Table 2) more than compensating for any suppressed response of TRW data to short-term temperature changes. Note also that the inter-annual standard deviation of the JJ temperature is 20% larger than for the JJA season used for the Yamalia reconstruction shown in Fig. 13a–e (the JJ version is shown in Fig. 13f for comparison).

Cooling is inferred from both reconstructions after some notable explosive volcanic eruptions. A full analysis of the link to volcanoes is beyond the scope of the present study, but we note that 1259 is a relatively cool year, though not extreme compared to other years and followed by a rapid return to warmer summer temperatures (Fig. 13b; see Mann et al., 2012; Anchukaitis et al., 2012). Some decadal or multi-decadal trends show close agreement between the reconstructions (e.g. 1300–1310, Fig. 13b; 1445–1455, Fig. 13c). The cool periods noted earlier (around 1450 and 1530) are examined in Fig. 13c, which indicates cooling of around 2–3 °C sustained for a decade or more in both reconstructions, so that they are particularly apparent in the smoothed data (Fig. 13d).

At the medium and longer timescales, the shapes of the two reconstructions are obviously similar due to the Yamal TRW data that are common to both (Fig. 13d–f). The amplitudes of the inferred changes and the uncertainty estimates are, however, different and depend upon the target season and calibration method. Using the JJA season and calibrating against the calibrated MXD data (see SM8), the Yamalia-Combined temperature reconstruction shows smaller changes (an average pre-industrial anomaly of about 0.5 °C compared with closer to 1.0 °C for Yamal-TRW) and greater uncertainty, such that significant cooling is much less apparent than for the Yamal-TRW case. The two estimates are in closer agreement when the JJ season is used, which is more appropriate for the TRW data that determine the medium and low frequencies of the reconstruction. The uncertainty range, even when using the JJ season, remains larger than for the Yamal-TRW reconstruction, because the Yamalia TRW chronology fits the instrumental temperatures less well at the 100-year timescale (principally the period of little temperature change during the early 20th century).

12. Discussion and conclusions

No tree-ring chronology, multiple chronology dataset, or climate reconstruction based on them should be considered final in the sense that they are "fixed in stone". Tree-ring chronologies evolve as additional sub-fossil data are located and more recent samples are collected in order to update the series. Different statistical processing approaches also allow a range of chronologies to be constructed, perhaps emphasising different timescales or geographic foci. In this review of the tree-ring evidence for past temperature changes in Yamalia, we have described the development of work in terms of improving data quantity and experimentation with different applications of RCS. The earliest RCS-based summer temperature reconstruction for this region (Briffa et al., 1995) concluded that the medieval period (the 11th and 12th centuries) was generally cool. It was apparent some time ago that this conclusion was based on the interpretation of too few

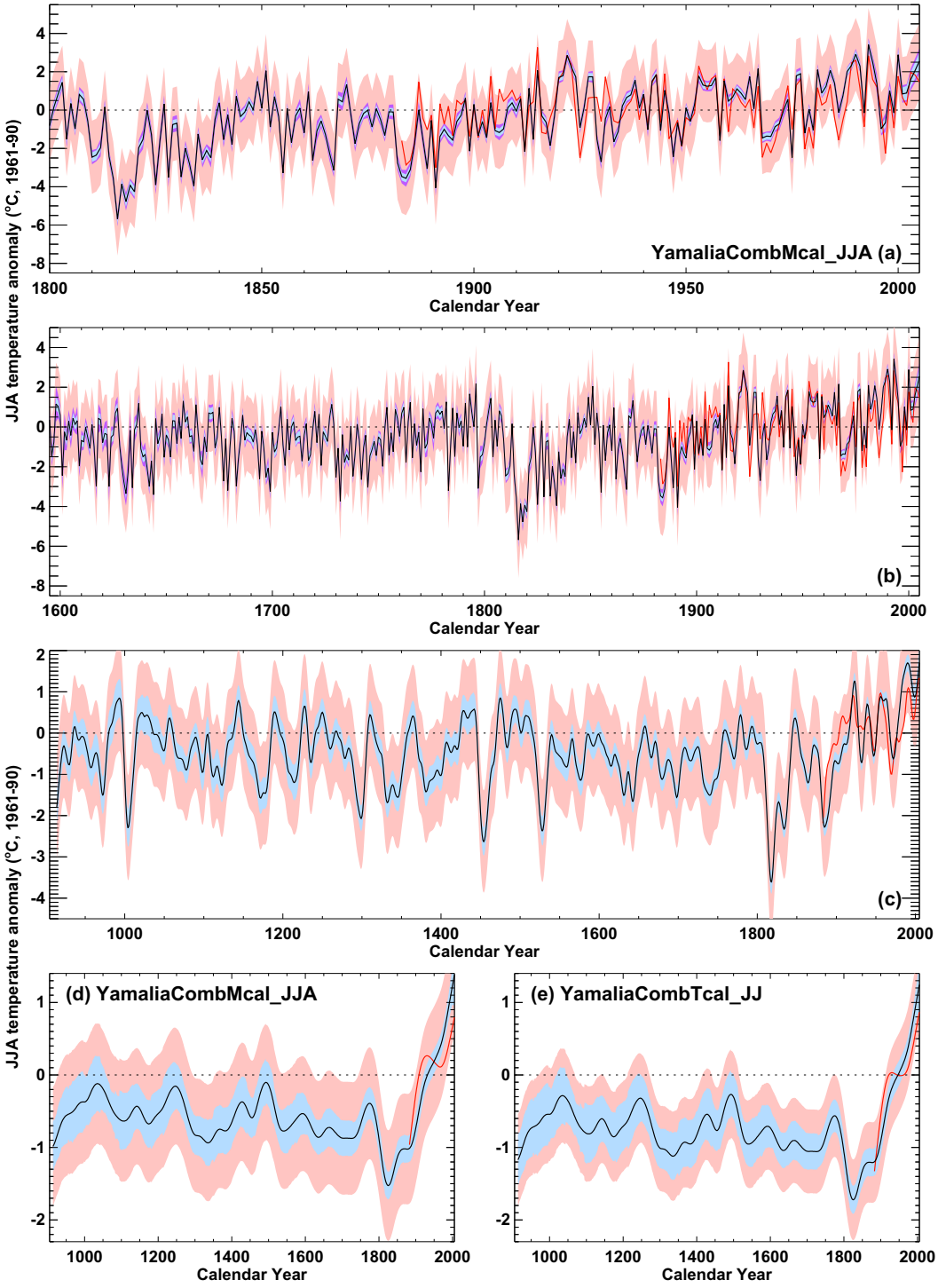

Fig. 12. As Fig. 11, but for the "Yamalia-Combined" temperature reconstructions based on the combined Yamalia TRW and Polar Urals MXD chronologies. In (a)–(d), the reconstruction is calibrated to represent the JJA season and the TRW is calibrated against the medium-frequency calibrated MXD data. In (e), the reconstruction is calibrated to represent the JJ season and the TRW is calibrated against the medium-frequency instrumental temperature data.

MXD data representing medieval time, and later analyses of more numerous TRW data from the adjacent Yamal area (Briffa, 2000) indicated that, on the contrary, there were two short 'warm' periods either side of 1000 CE. While this specific analysis showed the medieval level of tree growth rate was above the long-term average it also suggested that it was likely below the modern (post 1920) level. A simple, one-curve RCS version of the poorly-replicated Polar Urals (Pou-la.trw only) TRW shown in Fig. 7 of Briffa et al. (1996) showed medieval and late 15th and late 16th century tree growth to be higher than in the 20th century, but the 15th and 16th centuries contained some root-collar-derived data and the most recent data came from a single site with comparatively low-growth rate, as more recently acquired modern data from a number of sites has now revealed.

The first RCS Yamal TRW chronology and its subsequent "evolution" have maintained a generally consistent picture of implied

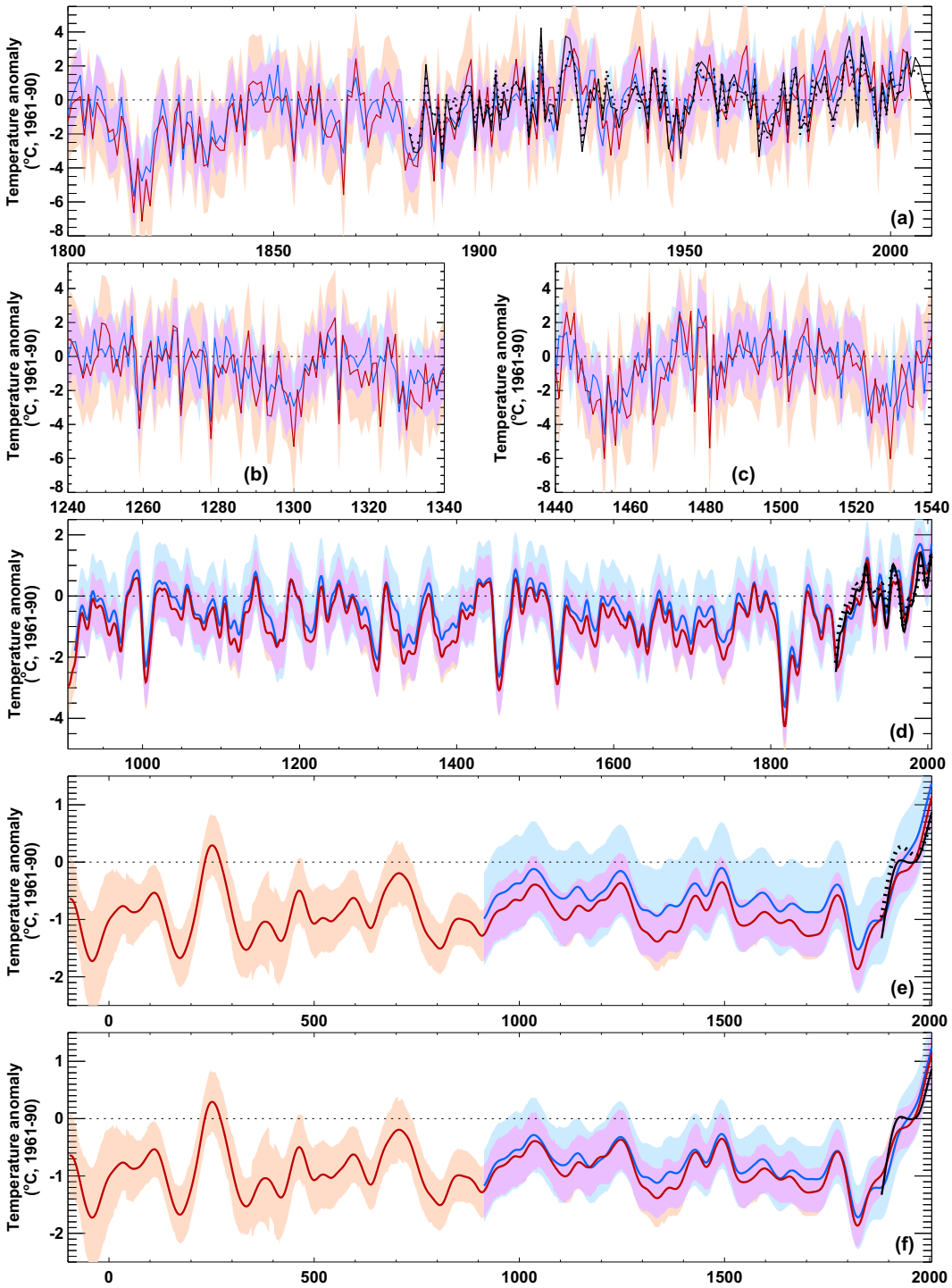

Fig. 13. Comparison of the "Yamal-TRW" (red lines; orange shading) and "Yamalia-Combined" (blue lines and shading) temperature reconstructions and their confidence intervals (overlap shading in purple). For "Yamalia-Combined", the JJA reconstruction presented in Fig. 12a–d is shown in (a–e) together with the JJA instrumental temperatures (black dotted line), while the JJ reconstruction presented in Fig. 12e is shown in (f). The JJ instrumental temperatures are shown in all panels (black solid line). Unfiltered reconstructions for (a) 1800–2005, (b) 1240–1340; and (c) 1440–1540; (d) 15-year smoothed reconstruction for 905–2005; and (e–f) 100-year smoothed from –96 onwards. Note that the smoothed values at the ends of the series are much more uncertain due to the presence of end effects on the spline filters, especially for (e–f). (For interpretation of the references to colour in this figure legend, the reader is referred to the web version of this article.)

Common-Era anomalous warm and cool periods, though clearly the earlier inferences, based on fewer samples, were less reliable. These analyses (Briffa, 2000; Briffa et al., 2008; Briffa and Melvin, 2009) indicated that post 1920 levels of tree growth and inferred summer warmth were likely the highest of the last 2000 years. The most recent analysis we describe here (Fig. 10), constitutes a "conservative approach" to the representation of what is still shown to be a generally high level of 20th century tree growth. The RCS application we have used, i.e. two-curve, signal-free RCS has reduced the potential influence of "modern sample bias" that might otherwise exaggerate 20th and 21st century levels in the TRW data. Whether this has overly suppressed the extent of the

"real" increase in modern tree growth (and to an extent reduced the scale of the lower growth of the 17th century) is unresolved. Similarly, the transformation of tree indices to have a normal distribution prior to their being averaged to form the chronology is shown to further reduce the apparent high level of tree growth in recent decades, merely because these recent values are among the most positive in the chronology series. Nevertheless, the application of RCS we have used and the associated chronology uncertainty allow us to re-state with some confidence that post-1920 tree growth in this region is significantly above the long-term average and likely higher than that in prior periods during the last 1700 years. There is a strong indication of notably high growth in the 3rd century CE (Fig. 9). Another earlier period of seemingly high growth and implied warmth (circa 450 BCE) must be considered far less reliable because of the comparatively few measurement series and high error associated with this part of the record. These inferences are consistent with conclusions pertaining to the precedence of recent temperatures for this region based on earlier published chronologies (Briffa, 2000; Briffa et al., 2008; Briffa and Melvin, 2009).

It is a challenge to maintain homogeneity of the constituent data sets when using RCS, particularly when updating series. We have demonstrated how large numbers of samples allow the division of the RCS data into sub-chronologies. Confidence in the interpretation of past tree-growth changes is raised if these exhibit common patterns of variability. For the first time, common high- and medium-frequency variability has been shown to exist across both the TRW and MXD chronology data in this region. We also reveal much common low-frequency variability between the Yamal and Polar Urals TRW chronologies and to a lesser extent with the Polar Urals MXD chronology over the last millennium.

We have noted that some recent large-scale climate reconstructions use a version of Polar Urals TRW chronology drawn from the RCS processing of a large, circum-hemispheric TRW data set described in Esper et al. (2002) and Cook et al. (2004). We have shown here that that version of the Polar Urals TRW chronology (also combining larch and spruce data) is biased by the inclusion of multiple root-collar-derived sample data. These wood samples are often larger, with comparatively wider annual rings than equivalent samples taken from higher in the same trees. RCS processing of these sample data produces erroneously large indices and the Polar Urals chronology containing them shows exaggerated growth levels and implies overly warm summer temperatures during medieval times (circa 900 to 1100 CE) and in the late 15th and early 16th centuries.

After removing these root-collar samples from the TRW data, and reprocessing the Polar Urals MXD to account for potential processing biases in data sets produced at different times or on different densitometry equipment, we show a largely compatible picture of long-timescale tree-growth changes over the last millennium in all Yamalia chronologies. However, both the currently available TRW and MXD data from the Polar Urals are less reliable in portraying low-frequency growth variability than are the currently available TRW data from Yamal. Even allowing for this, our current interpretation of all of the available Yamalia data indicate recent tree-growth levels that, when averaged over 25- or 100-year periods, are higher than previous levels observed in the last 2000 years. When averaged over 50-year periods, however, the modern growth levels are not significantly higher than those observed during one early (223–272 CE) section of the Yamalia chronology. Summer temperatures inferred from the Yamal chronology indicate that there is no statistically significant difference between the two warmest 50-year means (1955–2004 and 223–272 CE) but that it is likely that the last 100-year period (1906–2005) was warmer than any other century during the last 2000 years.

13. Concluding note

The various chronology series we present here provide largely compatible information regarding past tree-growth changes that lead to mutually-supportive inferences about the history of summer temperature changes in Yamalia. However, it would be wise to bear in mind a number of issues that amount to caveats when considering or using the temperature reconstruction data we provide. It is worth stressing that the specific climate history we present here relates only to the region from which the tree-ring data are drawn. There is no definitive prescription for how small or large such a region should be. Incorporating many (ideally homogeneous) data from a small region will allow more rigorous application of the RCS approach and enable more reliable inferences about past climate variability. Incorporating data from too wide a region will invariably "dilute" the common signal of tree growth by mixing trees that reflect different regional climate responses (see SM9). Whatever the geographic scale of data integration, every effort should be made to maintain the same spatial representation of sample data throughout the whole length of the chronology. Hence we add a cautionary note stressing the seasonality and local scale of the inferred climate history we present here: it represents summer temperature for Yamalia.

The long-timescale information contained in these reconstructions remains the least reliable component of their total variance. However, there is no evidence of "divergence", i.e. any late 20th century underperformance in tree productivity compared to that expected on the basis of increasing summer temperature (Briffa et al., 1998; D'Arrigo et al., 2008; Esper et al., 2009). We have not investigated the influence of sample elevation on the absolute magnitude of tree growth or made any allowance for such differences in our analysis, but this may not be a very significant factor (Briffa et al., 1996).

We also recognise that as temperatures have risen in this area during the 20th century, what were comparatively slow-growing near-timberline trees, possibly with low foliage density, might respond not just directly by increasing net productivity but also by increasing their needle mass, so enhancing their capacity to produce increasingly large amounts of growth material for the same temperature change. Persistent warming might also lead to other growth-promoting changes in the environment (e.g. increased soil mineralisation, nutrient recycling, or promotion of mycorrhizal activity) that could also conceivably promote tree growth beyond the degree expected as a linear response to the degree of warming. However, if this were true of the 20th century it would presumably also be true for earlier warm periods. Specific study of these issues in Yamalia will require further updated tree samples and continual monitoring of detailed climate and other environmental factors.

We end with the usual caveat that our interpretation of past tree growth changes in terms of varying summer temperatures relies on the assumption of uniformitarianism: that the same character and degree of association we observe now between tree growth and 20th century climate holds true throughout the length of our reconstructions and that no confounding factors have interfered with this relationship if the reconstructions are to be valid, within estimated uncertainty, for the last two millennia.

Acknowledgements

KRB, TMM and TJO acknowledge support from NERC (NE/G018863/1). RMH, AVK, VSM and SGS acknowledge support from

the partnership project of the Ural and Siberian Branches of the Russian Academy of Sciences (№ 12-C-4-1038 and № 69). SGS, VSM and RMH acknowledge support from the Russian Foundation for Basic Research (№ 11-04-00623-a, № 13-04-00961-a and № 13-04-02058).

Appendix A. Supplementary data

Supplementary data related to this article can be found at http://dx.doi.org/10.1016/j.quascirev.2013.04.008.

References

Anchukaitis, K.J., Breitenmoser, P., Briffa, K.R., Buchwal, A., Büntgen, U., Cook, E.R., D'Arrigo, R.D., Esper, J., Evans, M.N., Frank, D., Grudd, H., Gunnarson, B.E., Hughes, M.K., Kirdyanov, A.V., Körner, C., Krusic, P.J., Luckman, B., Melvin, T.M., Salzer, M.W., Shashkin, A.V., Timmreck, C., Vaganov, E.A., Wilson, R.J.S., 2012. Tree rings and volcanic cooling. Nature Geoscience 5, 836–837. http://dx.doi.org/10.1038/ngeo1645.

Barker, F., Soh, Y.C., Evans, R.J., 1988. Properties of the geometric mean functional-relationship. Biometrics 44, 279–281.

Bräker, O.U., 1981. Der Alterstrend bei Jahrringdichten und Jahrringbreiten von Nadelhölzern und sein Ausgleich. Mitteilungen der Forstlichen Bundesversuchsanstalt Wien 142, 75–102.

Briffa, K.R., 2000. Annual climate variability in the Holocene: interpreting the message of ancient trees. Quaternary Science Reviews 19, 87–105.

Briffa, K.R., Cook, E.R., 2008. Reducing and representing uncertainties in high-resolution proxy climate data. In: Workshop on Reducing and Representing Uncertainties in High Resolution Proxy Climate Data. PAGES/CLIVAR, Trieste, Italy.

Briffa, K.R., Jones, P.D., 1990. Basic chronology statistics and assessment. In: Cook, E.R., Kairiukstis, L.A. (Eds.), Methods of Dendrochronology. Kluwer Academic Publishers, pp. 137–152.

Briffa, K.R., Melvin, T.M., 2009. Examining the Validity of the Published RCS Yamal Tree-ring Chronology. Unpublished report. University of East Anglia, Norwich. http://www.cru.uea.ac.uk/cru/people/briffa/yamal2009/.

Briffa, K.R., Melvin, T.M., 2011. A closer look at Regional Curve Standardisation of tree-ring records: justification of the need, a warning of some pitfalls, and suggested improvements in its application. In: Hughes, M.K., Diaz, H.F., Swetnam, T.W. (Eds.), Dendroclimatology: Progress and Prospects. Springer Verlag, pp. 113–145.

Briffa, K.R., Jones, P.D., Bartholin, T.S., Eckstein, D., Schweingruber, F.H., Karlén, W., Zetterberg, P., Eronen, M., 1992. Fennoscandian Summers from AD 500: temperature changes on short and long timescales. Climate Dynamics 7, 111–119.

Briffa, K.R., Jones, P.D., Schweingruber, F.H., Shiyatov, S.G., Cook, E.R., 1995. Unusual 20th-century summer warmth in a 1,000-year temperature record from Siberia. Nature 376, 156–159.

Briffa, K.R., Jones, P.D., Schweingruber, F.H., Karlén, W., Shiyatov, S.G., 1996. Tree-ring variables as proxy-climate indicators: problems with low frequency signals. In: Jones, P.D., Bradley, R.S., Jouzel, J. (Eds.), Climatic Variations and Forcing Mechanisms of the Last 2000 Years. Springer-Verlag, Berlin, pp. 9–41.

Briffa, K.R., Schweingruber, F.H., Jones, P.D., Osborn, T.J., Shiyatov, S.G., Vaganov, E.A., 1998. Reduced sensitivity of recent tree-growth to temperature at high northern latitudes. Nature 391, 678–682.

Briffa, K.R., Shishov, V.V., Melvin, T.M., Vaganov, E.A., Grudd, H., Hantemirov, R.M., Eronen, M., Naurzbaev, M.M., 2008. Trends in recent temperature and radial tree growth spanning 2000 years across northwest Eurasia. Philosophical Transactions of the Royal Society B-Biological Sciences 363, 2271–2284.

Büntgen, U., Esper, J., Frank, D.C., Nicolussi, K., Schmidhalter, M., 2005. A 1052-year tree-ring proxy for Alpine summer temperatures. Climate Dynamics 25, 141–153.

Buntgen, U., Raible, C.C., Frank, D., Helama, S., Cunningham, L., Hofer, D., Nievergelt, D., Verstege, A., Timonen, M., Stenseth, N.C., Esper, J., 2011. Causes and consequences of past and projected Scandinavian summer temperatures, 500–2100 AD. PLoS ONE 6, e25133. http://dx.doi.org/10.1371/journal.pone.0025133.

Burger, G., Fast, I., Cubasch, U., 2006. Climate reconstruction by regression – 32 variations on a theme. Tellus Series A-Dynamic Meteorology and Oceanography 58, 227–235.

Cook, E.R., Briffa, K.R., Meko, D.M., Graybill, D.A., Funkhouser, G., 1995. The segment length curse in long tree-ring chronology development for paleoclimatic studies. Holocene 5, 229–237.

Cook, E.R., Palmer, J.G., D'Arrigo, R.D., 2002. Evidence for a 'Medieval Warm Period' in a 1,100 year tree-ring reconstruction of past austral summer temperatures in New Zealand. Geophysical Research Letters 29, Art-1667.

Cook, E.R., Esper, J., D'Arrigo, R.D., 2004. Extra-tropical Northern Hemisphere land temperature variability over the past 1000 years. Quaternary Science Reviews 23, 2063–2074.

Cook, E.R., Buckley, B.M., Palmer, J.G., Fenwick, P., Peterson, M.J., Boswijk, G., Fowler, A., 2006. Millennia-long tree-ring records from Tasmania and New Zealand: a basis for modelling climate variability and forcing, past, present and future. Journal of Quaternary Science 21, 689–699.

Cook, E.R., Palmer, J.G., Ahmed, M., Woodhouse, C.A., Fenwick, P., Zafar, M.U., Wahab, M., Khan, N., 2013. Five centuries of Upper Indus River flow from tree rings. Journal of Hydrology 486, 365–375.

D'Arrigo, R.D., Wilson, R.J.S., Jacoby, G.C., 2006. On the long-term context for late twentieth century warming. Journal of Geophysical Research-Atmospheres 111, D03103. http://dx.doi.org/10.1029/2005JD006352.

D'Arrigo, R.D., Wilson, R.J.S., Liepert, B., Cherubini, P., 2008. On the 'Divergence Problem' in Northern Forests: a review of the tree-ring evidence and possible causes. Global and Planetary Change 60, 289–305.

Erlandsson, S., 1936. Dendrochronological Studies. University of Upsala.

Esper, J., Cook, E.R., Schweingruber, F.H., 2002. Low-frequency signals in long tree-ring chronologies for reconstructing past temperature variability. Science 295, 2250–2253.

Esper, J., Cook, E.R., Krusic, P.J., Schweingruber, F.H., 2003. Tests of the RCS method for preserving low-frequency variability in long tree-ring chronologies. Tree-Ring Research 59, 81–98.

Esper, J., Frank, D.C., Wilson, R.J.S., Briffa, K.R., 2005. Effect of scaling and regression on reconstructed temperature amplitude for the past millennium. Geophysical Research Letters 32, L07711. http://dx.doi.org/10.1029/2004GL021236.

Esper, J., Frank, D., Buntgen, U., Verstege, A., Hantemirov, R.M., Kirdyanov, A.V., 2009. Trends and uncertainties in Siberian indicators of 20th century warming. Global Change Biology 16, 386–398.

Esper, J., Buntgen, U., Timonen, M., Frank, D.C., 2012. Variability and extremes of northern Scandinavian summer temperatures over the past two millennia. Global and Planetary Change 88-89, 1–9.

Fritts, H.C., 1976. Tree Rings and Climate. Academic Press, London.

Goosse, H., Crespin, E., Dubinkina, S., Loutre, M.F., Mann, M.E., Renssen, H., Sallaz-Damaz, Y., Shindell, D., 2012. The role of forcing and internal dynamics in explaining the "Medieval Climate Anomaly". Climate Dynamics 39, 2847–2866.

Graybill, D.A., Shiyatov, S.G., 1989. A 1009 year tree-ring reconstruction of mean June-July temperature deviations in the Polar Urals. In: Proc. Second US-USSR Symp. Air Pollution Effects on Vegetation Including Forest Ecosystems. USDA For. Serv., NFES, pp. 37–42.

Graybill, D.A., Shiyatov, S.G., 1992. Dendroclimatic evidence from the northern Soviet Union. In: Bradley, R.S., Jones, P.D. (Eds.), Climate Since A.D. 1500. Routledge, London, pp. 392–414.

Hantemirov, R.M., Shiyatov, S.G., 2002. A continuous multimillennial ring-width chronology in Yamal, northwestern Siberia. Holocene 12, 717–726.

Hantemirov, R.M., Surkov, A.Y., 1996. A 3243-year tree-ring reconstruction of climatic conditions for the north of West Siberia. In: Problems of General and Applied Ecology. Proceedings of Young Scientists Conference, Ekaterinburg, pp. 266–278.

Hegerl, G.C., Crowley, T.J., Allen, M., Hyde, W.T., Pollack, H.N., Smerdon, J., Zorita, E., 2007. Detection of human influence on a new, validated 1500-year temperature reconstruction. Journal of Climate 20, 650–666.

Helama, S., Vartiainen, M., Kolstrom, T., Peltola, H., Merilainen, J., 2008. X-ray microdensitometry applied to subfossil tree-rings: growth characteristics of ancient pines from the southern boreal forest zone in Finland at intra-annual to centennial time-scales. Vegetation History and Archaeobotany 17, 675–686.

Helama, S., Makarenko, N.G., Karimova, L.M., Kruglun, O.A., Timonen, M., Holopainen, J., Merilainen, J., Eronen, M., 2009. Dendroclimatic transfer functions revisited: Little Ice Age and Medieval Warm Period summer temperatures reconstructed using artificial neural networks and linear algorithms. Annales Geophysicae 27, 1097–1111.

Helama, S., Begin, Y., Vartiainen, M., Peltola, H., Kolstrom, T., Merilainen, J., 2012. Quantifications of dendrochronological information from contrasting microdensitometric measuring circumstances of experimental wood samples. Applied Radiation and Isotopes 70, 1014–1023.

Holland, M.M., Bitz, C.M., 2003. Polar amplification of climate change in coupled models. Climate Dynamics 21, 221–232.

Jones, P.D., Briffa, K.R., Osborn, T.J., Lough, J.M., van Ommen, T.D., Vinther, B.M., Luterbacher, J., Wahl, E.R., Zwiers, F.W., Mann, M.E., Schmidt, G.A., Ammann, C.M., Buckley, B.M., Cobb, K.M., Esper, J., Goosse, H., Graham, N., Jansen, E., Kiefer, T., Kull, C., Kuttel, M., Mosley-Thompson, E., Overpeck, J.T., Riedwyl, N., Schulz, M., Tudhope, A.W., Villalba, R., Wanner, H., Wolff, E., Xoplaki, E., 2009. High-resolution palaeoclimatology of the last millennium: a review of current status and future prospects. The Holocene 19, 3–49.

Jones, P.D., Lister, D.H., Osborn, T.J., Harpham, C., Salmon, M., Morice, C.P., 2012. Hemispheric and large-scale land-surface air temperature variations: an extensive revision and an update to 2010. Journal of Geophysical Research-Atmospheres 117, D05127. http://dx.doi.org/10.1029/2011JD017139.

Joshi, M., Hawkins, E., Sutton, R., Lowe, J., Frame, D., 2011. Projections of when temperature change will exceed 2 °C above pre-industrial levels. Nature Climate Change 1 (8), 407–412.

Ljungqvist, F.C., 2010. A new reconstruction of temperature variability in the extra-tropical northern hemisphere during the last two millennia. Geografiska Annaler Series A-Physical Geography 92A, 339–351.

Mann, M.E., Jones, P.D., 2003. Global surface temperatures over the past two millennia. Geophysical Research Letters 30, 1820. http://dx.doi.org/10.1029/2003GL017814.

Mann, M.E., Zhang, Z.H., Hughes, M.K., Bradley, R.S., Miller, S.K., Rutherford, S., Ni, F.B., 2008. Proxy-based reconstructions of hemispheric and global surface

temperature variations over the past two millennia. Proceedings of the National Academy of Sciences of the United States of America 105, 13252–13257.
Mann, M.E., Fuentes, J.D., Rutherford, S., 2012. Underestimation of volcanic cooling in tree-ring-based reconstructions of hemispheric temperatures. Nature Geoscience 5, 202–205. http://dx.doi.org/10.1038/ngeo1394.
McCarroll, D., Loader, N.J., Jalkanen, R., Gagen, M.H., Grudd, H., Gunnarson, B.E., Kirchhefer, A.J., Friedrich, M., Linderholm, H.W., Lindholm, M., Boettger, T., Los, S.O., Remmele, S., Kononov, Y.M., Yamazaki, Y.H., Young, G.H.F., Zorita, E., 2013. A 1200-year Multi-proxy Record of Tree Growth and Summer Temperature at the Northern Pine Forest Limit of Europe. Holocene 23, 471–484. http://dx.doi.org/10.1177/0959683612467483.
Melvin, T.M., 2004. Historical Growth Rates and Changing Climatic Sensitivity of Boreal Conifers. Thesis. University of East Anglia, Norwich. http://www.cru.uea.ac.uk/cru/pubs/thesis/2004-melvin/.
Melvin, T.M., Briffa, K.R., 2008. A "signal-free" approach to dendroclimatic standardisation. Dendrochronologia 26, 71–86. http://dx.doi.org/10.1016/j.dendro.2007.12.001.
Melvin, T.M., Briffa, K.R., 2013a. CRUST: software for the implementation of Regional Chronology Standardisation: part 1, signal-free RCS. Dendrochronologia (submitted for publication).
Melvin, T.M., Briffa, K.R., 2013b. CRUST: software for the implementation of Regional Chronology Standardisation: part 2, further RCS options and recommendations. Dendrochronologia (in preparation).
Melvin, T.M., Grudd, H., Briffa, K.R., 2013. Potential bias in "updating" tree-ring chronologies using Regional Curve Standardisation: re-processing 1500-years of Torneträsk density and ring-width data. Holocene 23, 364–373.
Moberg, A., Brattstrom, G., 2012. Prediction intervals for climate reconstructions with autocorrelated noise-An analysis of ordinary least squares and measurement error methods. Palaeogeography Palaeoclimatology Palaeoecology 308, 313–329.
Naurzbaev, M.M., Vaganov, E.A., Sidorova, O.V., Schweingruber, F.H., 2002. Summer temperatures in eastern Taimyr inferred from a 2427-year late-Holocene tree-ring chronology and earlier floating series. Holocene 12, 727–736.
Osborn, T.J., Briffa, K.R., 2004. The real color of climate change? Science 306, 621–622.
Peters, K., Cook, E.R., 1981. The Cubic Smoothing Spline as a Digital Filter. Technical Report #CU-1-81/TR1. Lamont-Doherty Geological Observatory of Columbia University, New York.
Polge, H., 1966. Etablissement des courbes de variation de la densité du bois par exploration densitométrique de radiographies d'échantillons prélevés à la tarière sur des arbres vivants. Application dans les domaines technologique et physiologique. Annals of Forest Science 23, 1–206.
Schurer, A., Hegerl, G., Mann, M.E., Tett, S.F.B., Phipps, S.J., 2013. Separating forced from chaotic climate variability over the last millennium. Journal of Climate. http://dx.doi.org/10.1175/JCLI-D-12-00826.1.
Schweingruber, F.H., Briffa, K.R., 1996. Tree-ring density networks for climate reconstruction. In: Jones, P.D., Bradley, R.S., Jouzel, J. (Eds.), Climatic Variations and Forcing Mechanisms of the Last 2000 Years. Springer-Verlag, Berlin, pp. 43–66.
Schweingruber, F.H., Fritts, H.C., Bräker, O.U., Drew, L.G., Schar, E., 1978. The X-ray technique as applied to dendroclimatology. Tree-Ring Bulletin 38, 61–91.
Serreze, M.C., Barrett, A.P., Stroeve, J.C., Kindig, D.N., Holland, M.M., 2009. The emergence of surface-based Arctic amplification. The Cryosphere 3, 11–19.
Shi, F., Yang, B., Ljungqvist, F.C., Yang, F.M., 2012. Multi-proxy reconstruction of Arctic summer temperatures over the past 1400 years. Climate Research 54, 113–128.
Shiyatov, S.G., 1962. The upper treeline in the Polar Urals and its dynamics in connection with climate changes. In: First Scientific Conference of Young Biological Specialists. Institute of Biology of the Ural Branch of the USSR Academy of Sciences, Sverdlovsk, pp. 37–48 (in Russian).
Shiyatov, S.G., 1986. Dendrochronology in the Upper Tree Line in the Urals. Nauka, Moscow, p. 136 (in Russian).
Shiyatov, S.G., 1993. The upper timberline dynamics during the last 1100 years in the Polar Ural Mountains. In: Frenzel, B. (Ed.), Oscillations of the Alpine and Polar Tree Limits in the Holocene. Gustav Fischer Verlag, Stuttgart, pp. 195–203.
Shiyatov, S.G., 1995. Reconstruction of climate and the upper timberline dynamics since AD 745 by tree-ring data in the Polar Ural Mountains. In: International Conference on Past, Present and Future Climate. Publication of the Academy of Finland, Helsinki, Finland, pp. 144–147.
Shiyatov, S.G., 2009. Dynamics of Wood and Shrub Vegetation in the Polar Ural Mountains under the Influence of Modern Climate Change. UB RAS, Ekaterinburg. ISBN: 978-5-7691-2035-0.
Tingley, M.P., Craigmile, P.F., Haran, M., Li, B., Mannshardt, E., Rajaratnam, B., 2012. Piecing together the past: statistical insights into paleoclimatic reconstructions. Quaternary Science Reviews 35, 1–22.
von Storch, H., Zorita, E., Jones, J.M., Dimitriev, Y., Gonzalez-Rouco, F., Tett, S.F.B., 2004. Reconstructing past climate from noisy data. Science 306, 679–682.
Wigley, T.M.L., Briffa, K.R., Jones, P.D., 1984. On the average value of correlated time series with applications in dendroclimatology and hydrometeorology. Journal of Climate & Applied Meteorology 23, 201–213.